TECHNICAL NOTES

NATIONAL ADVISORY COMMITTEE FOR AERONAUTICS

No. 759

PRESSURE-DISTRIBUTION INVESTIGATION OF AN N.A.C.A. 0009 AIRFOIL WITH A 30-PERCENT-CHORD PLAIN FLAP AND THREE TABS

By Milton B. Ames, Jr., and Richard I. Sears
Langley Memorial Aeronautical Laboratory

Washington
May 1940

NATIONAL ADVISORY COMMITTEE FOR AERONAUTICS

TECHNICAL NOTE NO. 759

PRESSURE-DISTRIBUTION INVESTIGATION OF AN N.A.C.A. 0009 AIRFOIL WITH A 30-PERCENT-CHORD PLAIN FLAP AND THREE TABS

By Milton B. Ames, Jr., and Richard I. Sears

SUMMARY

Pressure-distribution tests of an N.A.C.A. 0009 airfoil with a 30-percent-chord plain flap and three plain tabs, having chords 10, 20, and 30 percent of the flap chord, were made in the N.A.C.A. 4- by 6-foot vertical tunnel. The purpose of these tests was to continue an investigation to supply structural and aerodynamic section data that may be applied to the design of horizontal and vertical tail surfaces.

The results are presented as diagrams of resultant pressures and of resultant-pressure increments for the airfoil with the flap and the 20-percent-chord tab. Increments of normal-force and hinge-moment coefficients for the airfoil, the flap, and the three tabs are also given.

At all unstalled flap and tab deflections, the experimental distributions agree well with those calculated by an analytical method. The agreement is poor, however, when the stalled or the unstalled condition of the flap or the tab deflected alone was changed to an unstalled or stalled condition by the simultaneous deflection of both the flap and the tab.

INTRODUCTION

The trailing-edge tab has proved to be an effective device in reducing the excessive control forces resulting from the recent increases in size and speed of airplanes. Although a number of investigations have been conducted to determine the characteristics of the different factors

affecting control surfaces (references 1, 2, and 3), no data giving the aerodynamic section characteristics of a thin airfoil as affected by flaps and tabs seemed to be available that would be applicable to tail-surface design. An investigation was therefore undertaken to supply information applicable to the aerodynamic and the structural design of tail surfaces with tabs. The first part of this investigation comprised pressure-distribution tests made of an N.A.C.A. 0009 airfoil with a 50-percent-chord plain flap and three plain tabs; the results of these tests are reported in reference 4.

The results reported herein were obtained from pressure-distribution determinations over one section of an N.A.C.A. 0009 airfoil with a 30-percent-chord plain flap and with plain tabs 10, 20, and 30 percent of the flap chord. From the data obtained, normal-force and pitching-moment coefficients were calculated for the airfoil section complete with the flap and the various tabs. The normal-force and the hinge-moment coefficients for the flap with the different tabs and for the tabs separately were also determined.

APPARATUS AND TESTS

Model and Test Installation

The tests were made in the N.A.C.A. vertical wind tunnel. The test section of this tunnel has been converted from the original open, circular, 5-foot-diameter jet (reference 5) to a closed, rectangular, 4- by 6-foot throat shown in figure 1.

The rectangular 3-foot-chord by 4-foot-span model was made of laminated mahogany to the N.A.C.A. 0009 profile. It was equipped with a plain flap having a chord 30 percent of the airfoil chord, c, and with three serially hinged plain tabs having chords 10, 20, and 30 percent of the flap chord, c_f, as shown in figure 2. During tests, all flap and tab gaps were sealed with plasticine and cellulose tape to prevent air leakage at the hinges. The radius of curvature at the hinge for both the flap and the tabs was approximately one-half the airfoil thickness at the respective hinge positions.

A single chordwise row of pressure orifices was built

into the upper and the lower surfaces of the airfoil, the flap, and the tabs at the midspan. The orifice positions are shown in figure 3.

As the model completely spanned the test section, two-dimensional flow was approximated. The model was attached to the balance frame by means of torque tubes, which extended through the sides of the tunnel and were rotated by a calibrated electric drive to set the angle of attack. The flap and the tab angles were set inside the tunnel by varying the position of small lever arms on the movable surfaces.

The rubber tubes from the pressure orifices were brought out of the model at one end through the torque tube and the tunnel wall to a photographically recording multiple-tube manometer.

Tests

Tests were conducted at an effective Reynolds Number of approximately 3,410,000. (Effective Reynolds Number = test Reynolds Number × turbulence factor. The turbulence factor of the 4- by 6-foot vertical tunnel is 1.93.) The tunnel was operated at an average dynamic pressure of 10.8 pounds per square foot, corresponding to an air speed of about 65 miles per hour at standard sea-level conditions.

For direct comparison with the results presented in reference 4, the tests were made at angles of attack from $-14\frac{1}{2}^\circ$ to $10\frac{1}{2}^\circ$ at intervals of 5°. The model was tested with the 30-percent-chord plain flap deflected 0°, 5°, 10°, 20°, 30°, and 45°. Throughout the entire angle-of-attack range for each flap deflection, the three tabs were deflected 0°, $\pm 10^\circ$, $\pm 20^\circ$, and $\pm 30^\circ$.

RESULTS

Presentation of Data

The results of the distribution of pressures are given in the form of diagrams of resultant pressures and resultant-pressure increments, which represent changes in resultant-pressure distribution caused by a change in angle of any one part or any combination of the component

parts of the airfoil. The resultant normal pressure at any point along the chord line of the airfoil was determined by taking the algebraic difference of the pressures normal to the surface of the airfoil at that point. All diagrams of resultant pressures or resultant-pressure increments of the airfoil, flap, and tab combination are plotted as pressure coefficients, P, or as ΔP, where

$$P = \frac{p - p_o}{q}$$

and

p static pressure at a point on airfoil.

p_o static pressure in free air stream.

q dynamic pressure of free air stream.

Resultant-pressure diagrams are given for the basic section (i.e., flap and tab neutral) in figure 4. The resultant-pressure diagram for any other condition may be obtained by adding to the basic diagram the resultant-pressure-increment diagram (figs. 5 to 10) for the particular condition.

The large quantity of data prohibited the inclusion of all the resultant-pressure-increment diagrams. Only the diagrams for tab deflections of 0° and ±30° for the $0.20c_f$ tab, which was considered to be an average size, are presented. Values of angle of attack were selected to represent the following conditions:

Unstalled negative angle of attack ....$-9\frac{1}{2}^\circ$

Low positive angle of attack ..... $\frac{1}{2}^\circ$

Unstalled high angle of attack ..... $5\frac{1}{2}^\circ$

The angle of $5\frac{1}{2}^\circ$ was selected because it was the highest unstalled angle obtained at some of the higher flap and tab deflections and because the results could be compared with those presented in reference 4.

The section characteristics of the airfoil, the flap, and the tab, as functions of flap and tab deflection, are also plotted as increments. These increments were obtained by deducting the basic section coefficients from those for

the section with the tab, the flap, or the combination deflected. The characteristics were obtained in each case by mechanical integration of the original plotted pressure diagrams.

Computations were made to determine the section coefficients, which are defined as follows:

$c_n = \frac{n}{qc}$ airfoil section normal-force coefficient.

$c_m = \frac{m}{qc^2}$ airfoil section pitching-moment coefficient about quarter-chord point of airfoil.

$c_{n_f} = \frac{n_f}{qc_f}$ flap section normal-force coefficient.

$c_{h_f} = \frac{h_f}{qc_f^2}$ flap section hinge-moment coefficient.

$c_{n_t} = \frac{n_t}{qc_t}$ tab section normal-force coefficient,

$c_{h_t} = \frac{h_t}{qc_t^2}$ tab section hinge-moment coefficient.

where the forces and moments per unit span are:

n normal force of airfoil section.

m pitching moment of airfoil section about the quarter-chord point.

n_f normal force of flap section.

h_f hinge moment of flap section.

n_t normal force of tab section.

h_t hinge moment of tab section.

and c chord of basic airfoil with flap and tab neutral.

c_f flap chord.

c_t tab chord.

α angle of attack.

δ flap or tab deflection.

The subscript f refers to the flap with the tab; and the subscript t, to the tab alone.

The integrated coefficients for the basic airfoil are plotted against angle of attack in figure 11. The increments for various tab and flap deflections are presented in figures 12 to 20.

Precision

Inasmuch as no air-flow alinement tests have been made in this tunnel, the absolute value of the angle of attack is not known. An error of $1/2^{\circ}$ in alinement appeared to have existed (see reference 4); corrections for this misalinement were made in the final data. Relative angles of attack are accurate to within $\pm 0.1^{\circ}$. Absolute flap and tab deflections were set to $\pm 2^{\circ}$; their relative settings are accurate to within $\pm 1^{\circ}$.

Plotted pressures are correct to within ± 2 percent except at the peaks that occurred at the hinge axes and at the nose, where the variation may be greater. The dynamic-pressure readings are accurate to within ± 1 percent.

Two-dimensional flow having been approximated, the results may be considered as section characteristics except for the tunnel-restriction corrections which were applied only to the airfoil section normal-force coefficient, c_n. Although no corrections were made for the other coefficients, they are believed to be higher than the free-air values and, hence, are on the conservative side for structural purposes. The magnitude of tunnel corrections for flap and tab coefficients has not been determined. The magnitude of the airfoil normal-force coefficient as represented in the resultant-pressure-increment diagrams (figs. 5 to 10) is known to be too large by about 11 percent because these curves were plotted directly from tunnel data without applying any correction.

DISCUSSION

Pressure Distribution

The distribution of resultant pressure for the basic N.A.C.A. 0009 airfoil with flap and tabs neutral (fig. 4) and the distribution over the basic section of increments of resultant pressure caused by flap and tab deflections (figs. 5 to 10) are uncorrected for tunnel effect. Such diagrams should prove useful in determining loading conditions for the structural design of both horizontal and vertical tail surfaces. For this purpose, all pressures are conservative. This conclusion is especially true of the peaks at the hinge axes because of the use of sealed gaps.

Tests have indicated that the increments of pressure distribution and the increments of section aerodynamic coefficients due to flap deflection are approximately independent of the basic section for conventional airfoils of the same maximum thickness. It is therefore believed that, for structural design, the incremental data presented in this report may be applied to other basic sections of a conventional shape and the same thickness.

Deflection of the flap alone or the tab alone causes an increment of pressure over the entire airfoil, this increment reaching peak values both at the nose and at the hinge axis. The increment tapers from this peak value at the hinge axis to zero at the trailing edge. When the flap and the tab are simultaneously deflected in the same direction, the increments are largest; peaks occur at the same places and reach their maximum values. If the flap and the tab are deflected simultaneously but in opposite directions, increments are a minimum; but peaks still occur at the nose and at the hinge axes. The peaks at the hinge axes are, however, of opposite sign. The resultant-pressure increment on the flap (flap deflected downward) is a positive peak at the flap hinge axis, passes through zero between the flap and the tab hinges, and reaches a negative peak at the tab axis (tab deflected upward), from which it drops to zero at the trailing edge of the airfoil.

In general, the curves of the resultant-pressure increments are similar in form to those for the 50-percent-chord flap of reference 4. As might be expected, the 30-

percent-chord flap stalls at a higher angle of attack and its loads are smaller. The irregularities in some of the curves (figs. 5(a), 5(c), 6(c), 7(c), 8(a), 8(c), 9(c), and 10(c)) over the leading-edge portion of the airfoil may be due to laminar separation caused by severe adverse pressure gradients.

The curves of resultant-pressure distribution over the basic airfoil (fig. 4) are the same as those presented in figure 4 of reference 4. The comparison of the experimental curves with those obtained by a computed method are therefore omitted in this report.

Calculations were made for the chordwise distribution of pressure increments, resulting from flap and tab deflections, by the method advanced in reference 6. Comparisons with the experimental curves are shown in figures 5, 7, 8, and 9. The curves in these figures show this method of computing incremental pressure distributions to be in good agreement with experimental results for deflections at which the flap or tab alone was unstalled. Of the cases for which agreement may be considered satisfactory, the greatest divergence of the curves is $0.2\Delta P$ and occurs at the hinge axes (figs. 5(a) and 7(b)).

On the other hand, when the flap and the tab were simultaneously deflected in the same direction or in opposite directions and the flap, the tab, or both were stalled, the computed curves did not agree with the experimental curves. This result is in disagreement with other results cited in reference 6.

The method advanced in reference 6 is based upon the assumption that, at a given angle of attack, the coefficient increments Δc_n and Δc_m for the flaps deflected alone to a given angle plus the coefficient increments for the tab deflected alone to a given angle should equal the coefficient increments for flap and tab simultaneously deflected to these given angles. This assumption is not borne out by experiment in the following cases:

Flap deflection, 10°; angle of attack, $5\frac{1}{2}^\circ$; tab deflection, -30° (fig. 7(c)).

Flap deflection, 20°; angle of attack, $1/2^\circ$; tab deflection, -30° (fig. 8(b)).

Flap deflection, 30°; angle of attack, $1/2^\circ$; tab deflection, $\pm 30^\circ$ (fig. 9(b)).

This poor summation of coefficients is caused by the occurrence of a critical condition in which the stalled or the unstalled condition of either the flap or the tab deflected alone is changed by the simultaneous deflection of both the flap and the tab. The experiments show that, in some cases where the flap was stalled when deflected alone, the tab when deflected at the same time in the opposite direction caused the flap to become unstalled. In other tests, where both the flap and the tab were deflected in the same direction at the same time, the tab often became stalled and, in a number of cases, both the flap and the tab stalled. It is evident that the method of computing chordwise distribution, based on the summation of coefficients due to the flap and the tab deflections, will not check the experimental results where the stalled or the unstalled condition of the flap or the tab deflected alone was changed by the simultaneous deflection of the flap and tab. It should be noted here, however, that various free-flight tests have shown that, for these critical conditions, the stalls in free flight may not necessarily occur in the order that the tunnel tests have indicated.

Aerodynamic Section Characteristics

Airfoil characteristics.- The basic airfoil section gave a linear variation of c_n against angle of attack (fig. 11) in the unstalled range, which was similar to the results obtained in reference 4. The slope of the normal-force curve, $\partial c_n/\partial\alpha$, is 0.095 and agrees with the results in references 4 and 7. The failure of the c_n curves to give a value of $c_n = 0$ at $\alpha = 0$ was probably due to model imperfections and tab misalinement. The maximum increment of normal-force coefficient, $\Delta c_n = 1.73$, occurred at $\alpha = -9\frac{1}{2}^\circ$, $\delta_f = 45^\circ$, and $\delta_t = 30^\circ$ for the $0.30c_f$ tab. (See fig. 18(b).) When the tab was deflected upward to -30°, the other conditions remaining the same, the value of Δc_n became 1.06. The reduction of Δc_n due to reversing the tab was 0.67, or 39 percent. For the same condition in reference 4 where the model had a 0.50c flap, the maximum Δc_n was 2.32 for the tab deflection of 30° and 1.34 for the -30° tab deflection. The change in Δc_n in this case was 0.98, or about 42 percent for a 0.50 flap. In figures 12, 15, and 18, the Δc_n curves change slope at a flap deflection of 20° for negative angles of attack and between flap deflections of 10° and 20° for the positive angles of attack. These changes in slope are probably caused by the stalling of the flap.

The pitching-moment coefficient for the basic airfoil section was approximately zero for the range of angles of attack of $-9\frac{1}{2}^{\circ}$ to $10\frac{1}{2}^{\circ}$. (See fig. 11.) The value of c_m varied nearly linearly with flap deflection for all values of α within the unstalled range. It was noted that the effectiveness of the tabs in varying Δc_m decreased as tab deflections increased positively or negatively from the neutral position.

Flap and tab characteristics.- In agreement with reference 4, the increments of flap section normal-force and hinge-moment coefficients varied nearly linearly with flap deflection within the unstalled range of the flap. As would be expected, the flap stalled at successively lower flap deflections as the angle of attack was increased.

The curves of Δc_{n_f} and Δc_{h_f} were shifted parallel to themselves with different tab deflections. The rate of change of the increments with tab deflection decreased as the tab deflection increased positively or negatively from neutral. In most cases, the -30° (upward) deflection of the tab was rather ineffective in reducing Δc_{h_f}, as shown by the irregularity of the increments for this tab deflection. This result agrees with the results in references 1 and 2.

The incremental tab section coefficients, Δc_{n_t} and Δc_{h_t}, plotted in figures 14, 17, and 20, varied linearly with tab deflection through the unstalled range and were larger when the flap and the tab were deflected in the same direction than when they were deflected in opposite directions.

As indicated in the curves showing the flap-coefficient increments, the tab deflected -30° was stalled in most cases. In agreement with reference 4, at given values of α and δ_t, an increase in flap deflection caused increases in Δc_{n_t} and Δc_{h_t}. As the flap deflection was increased, the magnitude of the increases in Δc_{n_t} and Δc_{h_t} generally became larger. (See figs. 14, 17, and 20.)

The angle of attack for the curve of the flap deflected 30° in figure 14(f) is 9° instead of $10\frac{1}{2}^{\circ}$ as for the other flap deflections. Since the model in this condition was partly stalled, the flow was too unsteady for data to be taken at $\alpha = 10\frac{1}{2}^{\circ}$.

Comparison with Other Tests

In the following table are listed some of the more important average slopes obtained from this investigation. The comparisons are made with the experimental results from data in references 3 and 4. All slopes are corrected to infinite aspect ratio.

N.A.C.A. 0009 AIRFOIL

Source	Tunnel	Effective Reynolds Number	Flap chord (percent c)	$\partial c_n/\partial\alpha$	$\partial\alpha/\partial\delta_f$	$\left(\frac{\partial\delta_f}{\partial\alpha}\right)_{c_{h_f}=0}$	$\partial c_{h_f}/\partial\delta_f$	$\partial c_{h_f}/\partial\delta_t$	$\partial\alpha/\partial\delta_t$
This report	4- by 6-foot	3,410,000	30	0.095	0.57	-0.52	-0.014	[a]-0.013	[a]0.21
Reference 3	Full-scale	1,606,000	41	.083	.68	-.70	-.0096	[b]-.013	[b].25
Reference 4	4- by 6-foot	3,410,000	50	.095	.86	-.76	-.016	[a]-.016	[a].29

[a]Tab size, $0.20c_f$.

[b]Tab size, $0.195c_f$.

Two notable differences occur in this comparison between data from tests in the 4- by 6-foot vertical tunnel and in the full-scale tunnel. First, the value of $\partial c_n/\partial \alpha$ of 0.095 obtained from the present tests and those reported in reference 4, although not in accord with the value of 0.083 obtained in the tests reported in reference 3, is in agreement with the value of 0.095 from other full-scale-tunnel tests reported in reference 7. The other difference occurs in comparisons of values of $\partial c_{h_f}/\partial \delta_f$ and $\partial c_{h_f}/\partial \delta_t$. This difference is in accordance with expected results. As pointed out previously, the section characteristics of the flap and the tab herein reported were not corrected for tunnel effects. In addition, the gaps between the flap and the tab were sealed. Both of these factors would cause an increase in these slopes.

CONCLUDING REMARKS

Aerodynamic section characteristics and resultant-pressure distributions have been presented for the N.A.C.A. 0009 airfoil with a 30-percent-chord flap and three plain tabs having chords 10, 20, and 30 percent of the flap chord.

For all unstalled flap and tab deflections, the experimental and the calculated distributions of resultant-pressure increments are in good agreement.

The results of the analytical method of calculating the resultant-pressure distribution and the experimental results are not in agreement for the cases in which the stalled or the unstalled condition of the flap or the tab deflected alone was changed by the simultaneous deflection of the flap and the tab. This poor agreement between the experimental and the calculated results is attributed to the fact that the coefficient increments for these critical conditions are not additive, as they must be to obtain good agreement.

In the application of these data for design purposes, it should be remembered that, for all cases, gaps were completely sealed, resulting in higher peak pressures at the hinge axes and in higher hinge-moment and normal-force coefficients than would have been obtained with unsealed

gaps. It should also be noted that only the values of the normal-force coefficients were corrected for tunnel effects.

Langley Memorial Aeronautical Laboratory,
National Advisory Committee for Aeronautics,
Langley Field, Va., March 27, 1940.

REFERENCES

1. Wenzinger, Carl J.: Pressure Distribution over an Airfoil Section with a Flap and Tab. T.R. No. 574, N.A.C.A., 1936.

2. Harris, Thomas A.: Reduction of Hinge Moments of Airplane Control Surfaces by Tabs. T.R. No. 528, N.A.C.A., 1935.

3. Goett, Harry J., and Reeder, J. P.: Effects of Elevator Nose Shape, Gap, Balance, and Tabs on the Aerodynamic Characteristics of a Horizontal Tail Surface. T.R. No. 675, N.A.C.A., 1939.

4. Street, William G., and Ames, Milton B., Jr.: Pressure-Distribution Investigation of an N.A.C.A. 0009 Airfoil with a 50-Percent-Chord Plain Flap and Three Tabs. T.N. No. 734, N.A.C.A., 1939.

5. Wenzinger, Carl J., and Harris, Thomas A.: The Vertical Wind Tunnel of the National Advisory Committee for Aeronautics. T.R. No. 387, N.A.C.A., 1931.

6. Allen, H. Julian: Calculation of the Chordwise Load Distribution over Airfoil Sections with Plain, Split, or Serially Hinged Trailing-Edge Flaps. T.R. No. 634, N.A.C.A., 1938.

7. Goett, Harry J., and Bullivant, W. Kenneth: Tests of N.A.C.A. 0009, 0012, and 0018 Airfoils in the Full-Scale Tunnel. T.R. No. 647, N.A.C.A., 1938.

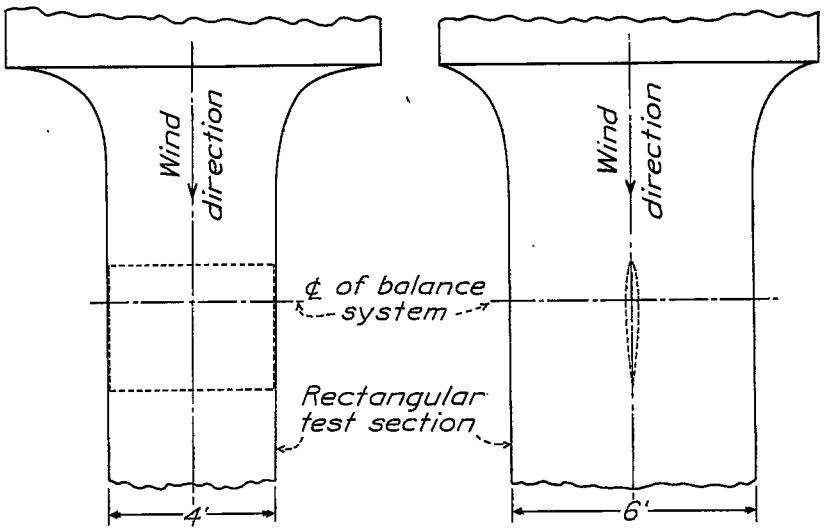

Figure 1.- Model mounted in 4-by 6-foot vertical tunnel.

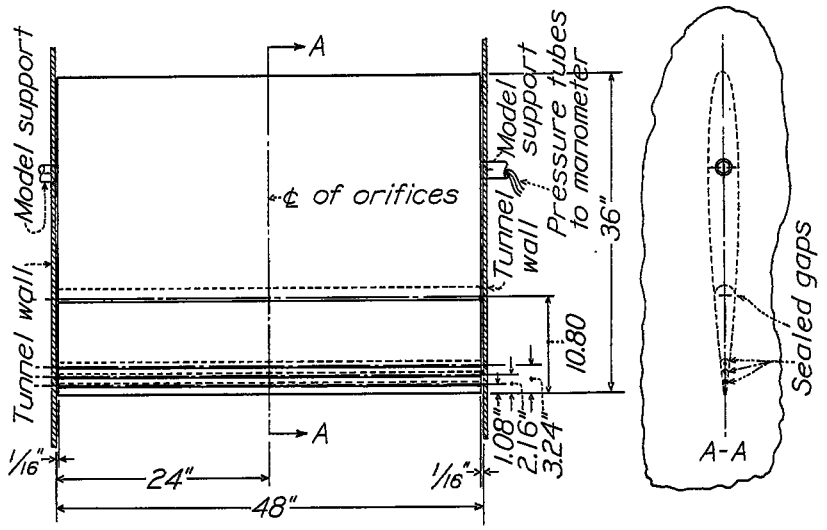

Figure 2.- The N.A.C.A. 0009 pressure-distribution model with 0.30c plain flap and 0.10cf, 0.20cf, and 0.30cf plain tabs.

Orifice	Location
0	0
1	.62
2	1.25
3	2.5
4	5.0
5	10.0
6	20.0
7	30.0
8	40.0
9	45.0
10	48.2
11	50.0
12	52.5
13	55.0
14	60.0
15	65.0
16	68.8
17	70.0
18	72.5
19	75.0
20	80.0
21	85.0
22	87.5
23	90.5
24	91.0
25	91.5
26	92.5
27	93.5
28	94.0
29	94.5
30	95.5
31	96.5
32	97.0
33	97.5
34	98.5
35	99.5

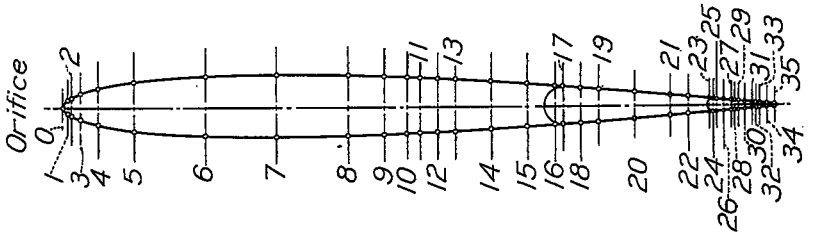

Figure 3.- Chordwise locations of pressure orifices on the N.A.C.A. 0009 airfoil in percent chord.

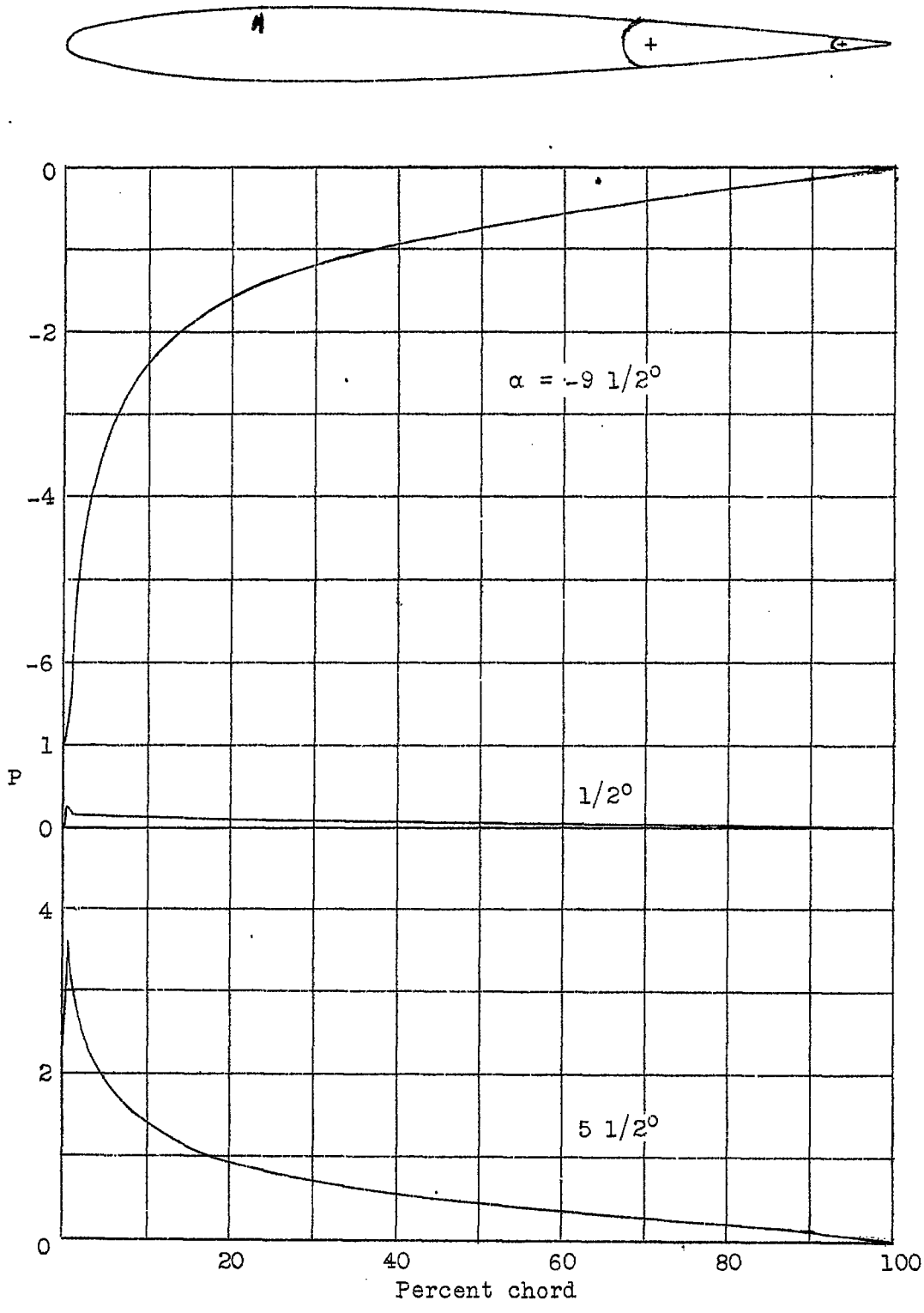

Figure 4.- Distribution of resultant pressure over the N.A.C.A. 0009 airfoil at various angles of attack. Flap and tab neutral.

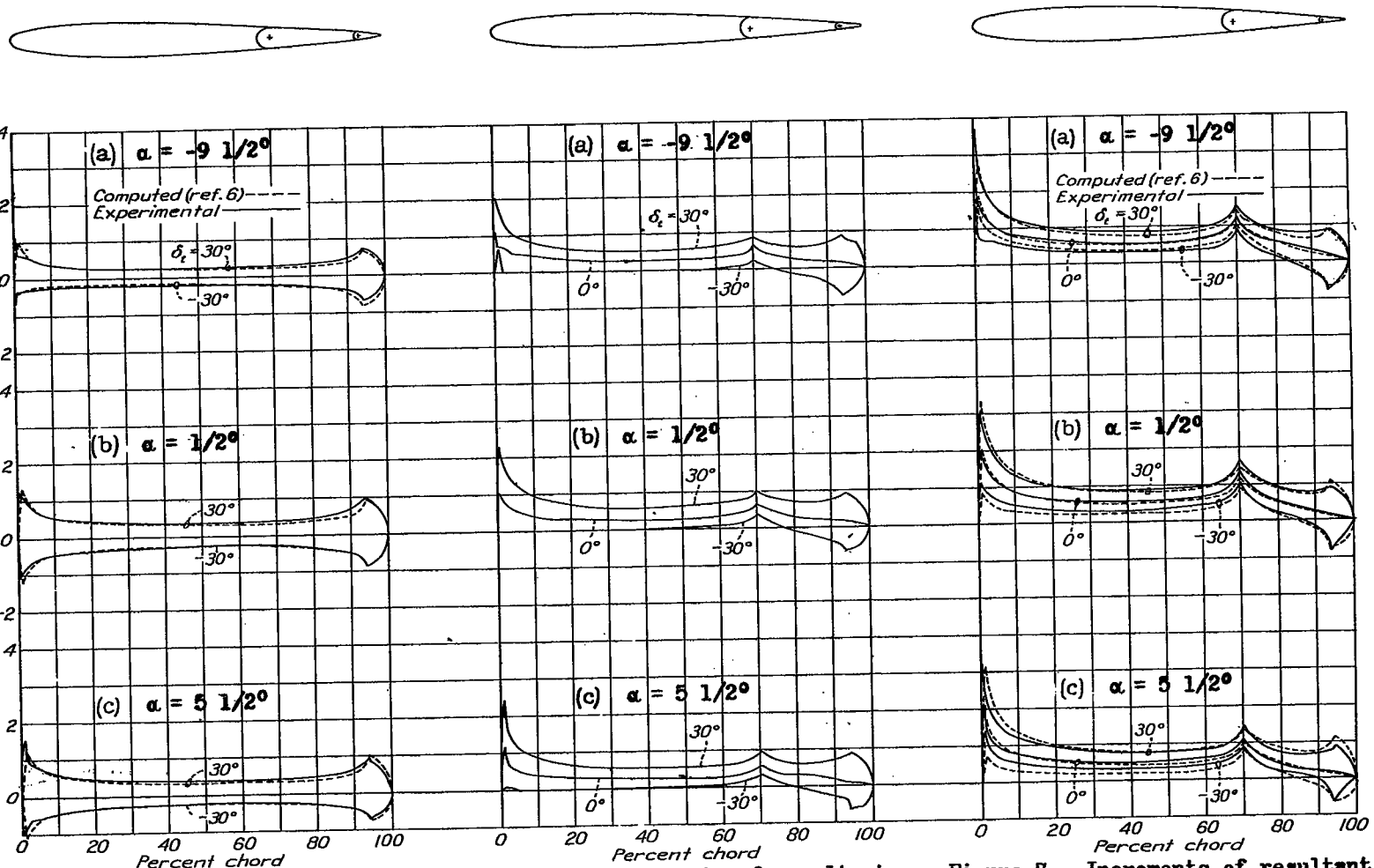

Figure 5.- Increments of resultant pressures for various angles of attack and various deflections of a 0.20c_f tab on a 0.30c plain flap deflected 0°.

Figure 6.- Increments of resultant pressures for various angles of attack and various deflections of a 0.20c_f tab on a 0.30c flap deflected 5°.

Figure 7.- Increments of resultant pressures for various angles of attack and various deflections of a 0.20c_f tab on a 0.30c flap deflected 10°.

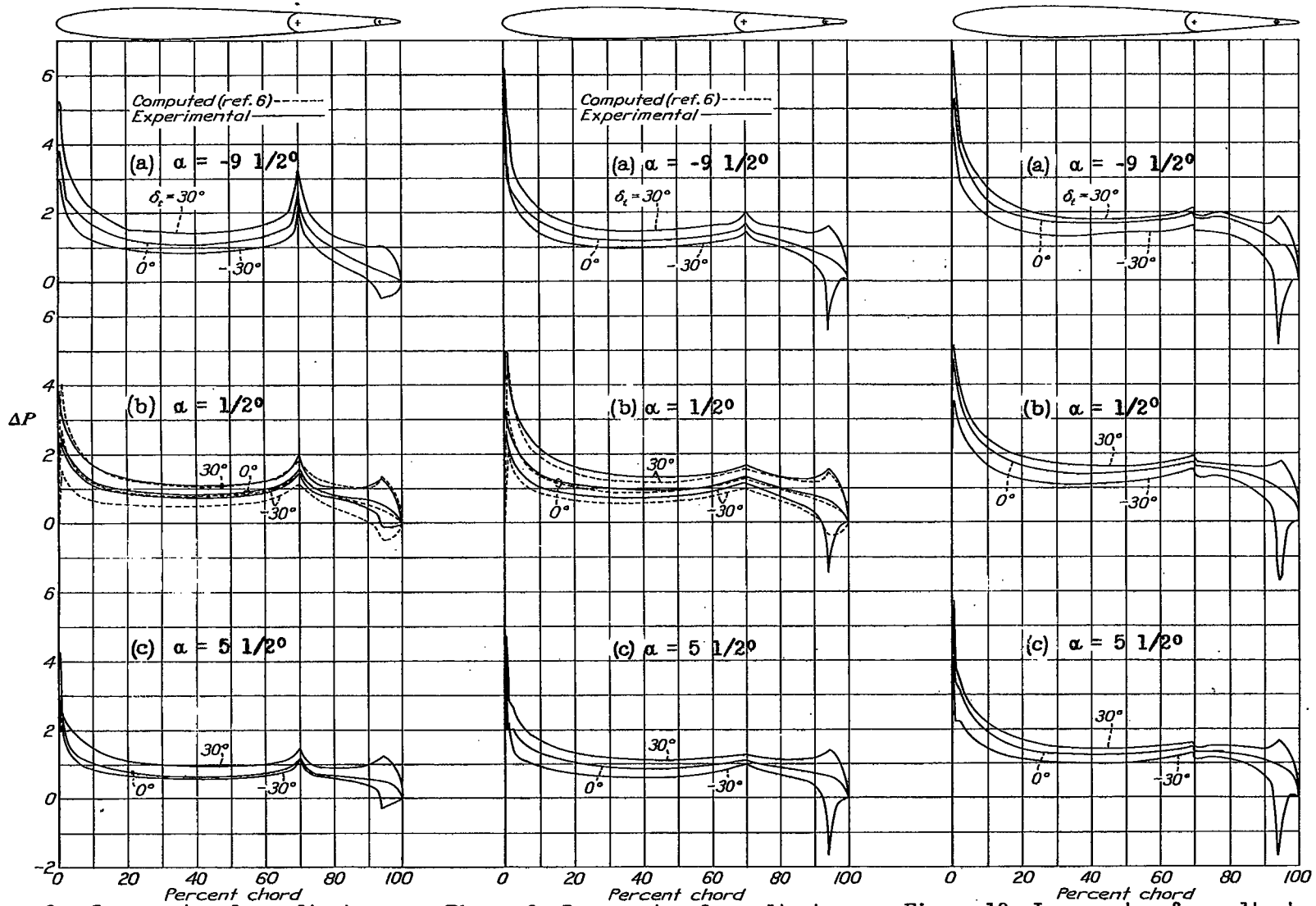

Figure 8.- Increments of resultant pressures for various angles of attack and various deflections of a 0.20c_f tab on a 0.30c flap deflected 20°.

Figure 9.-Increments of resultant pressures for various angles of attack and various deflections of a 0.20c_f tab on a 0.30c flap deflected 30°.

Figure 10.-Increments of resultant pressures for various angles of attack and various deflections of a 0.20c_f tab on a 0.30c flap deflected 45°.

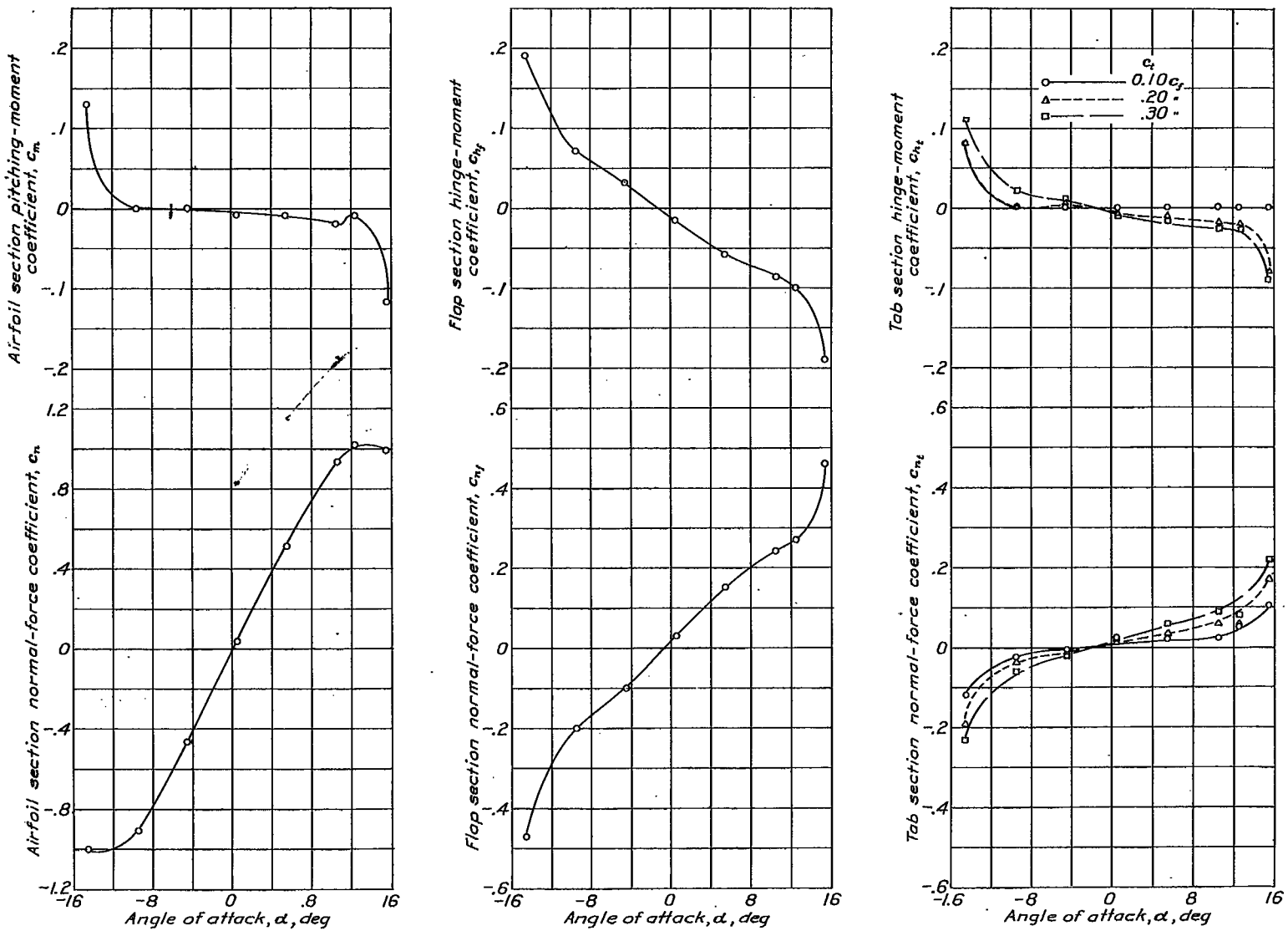

Figure 11.- Section characteristics of basic N.A.C.A. 0009 airfoil with 0.30c plain flap and tabs neutral.

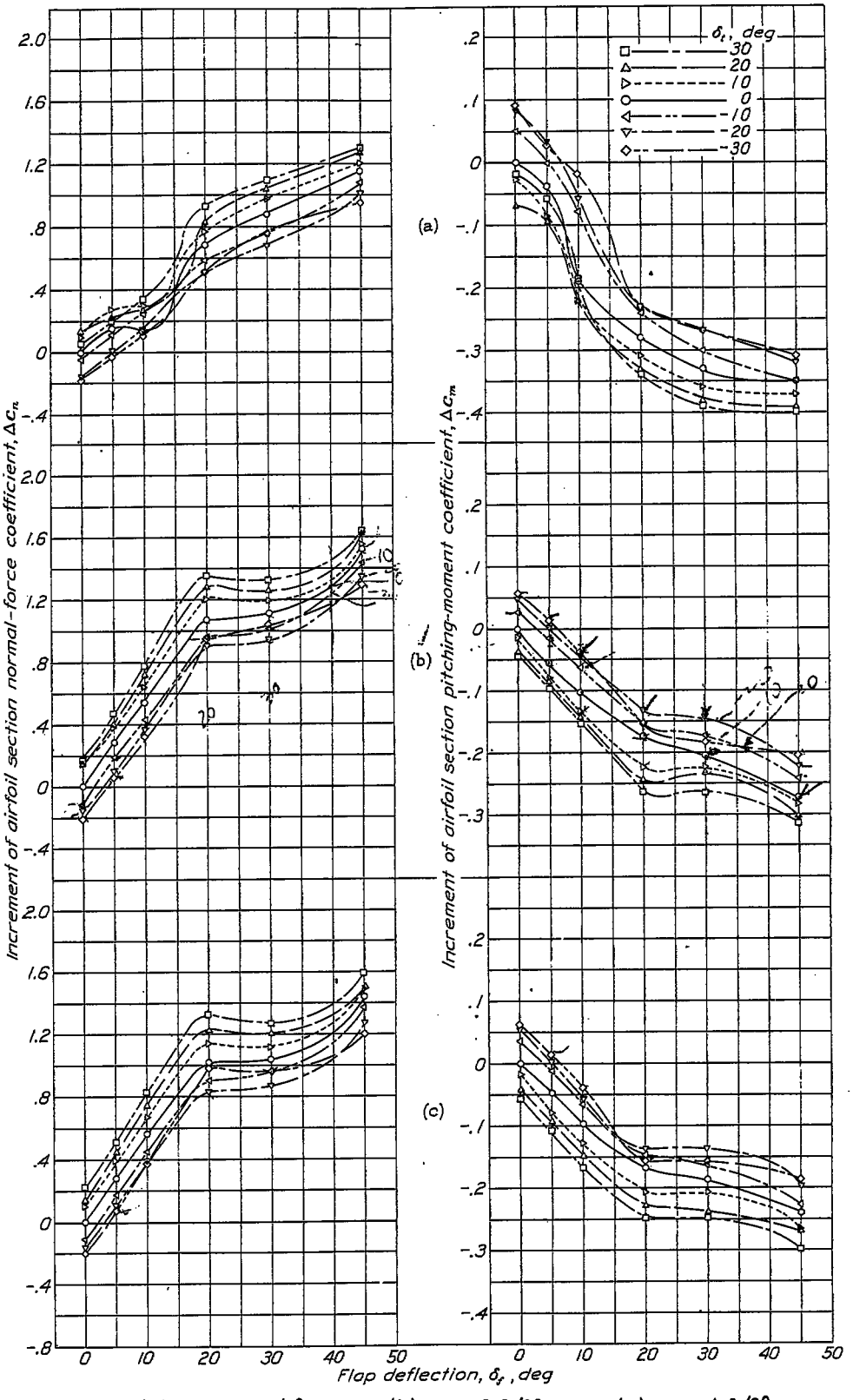

(a) α = -14 1/2° (b) α = -9 1/2° (c) α = -4 1/2°

Figure 12, a to f.- Increments of airfoil section normal-force and pitching-moment coefficients for various deflections of a 0.30c plain flap and a 0.10c_f tab.

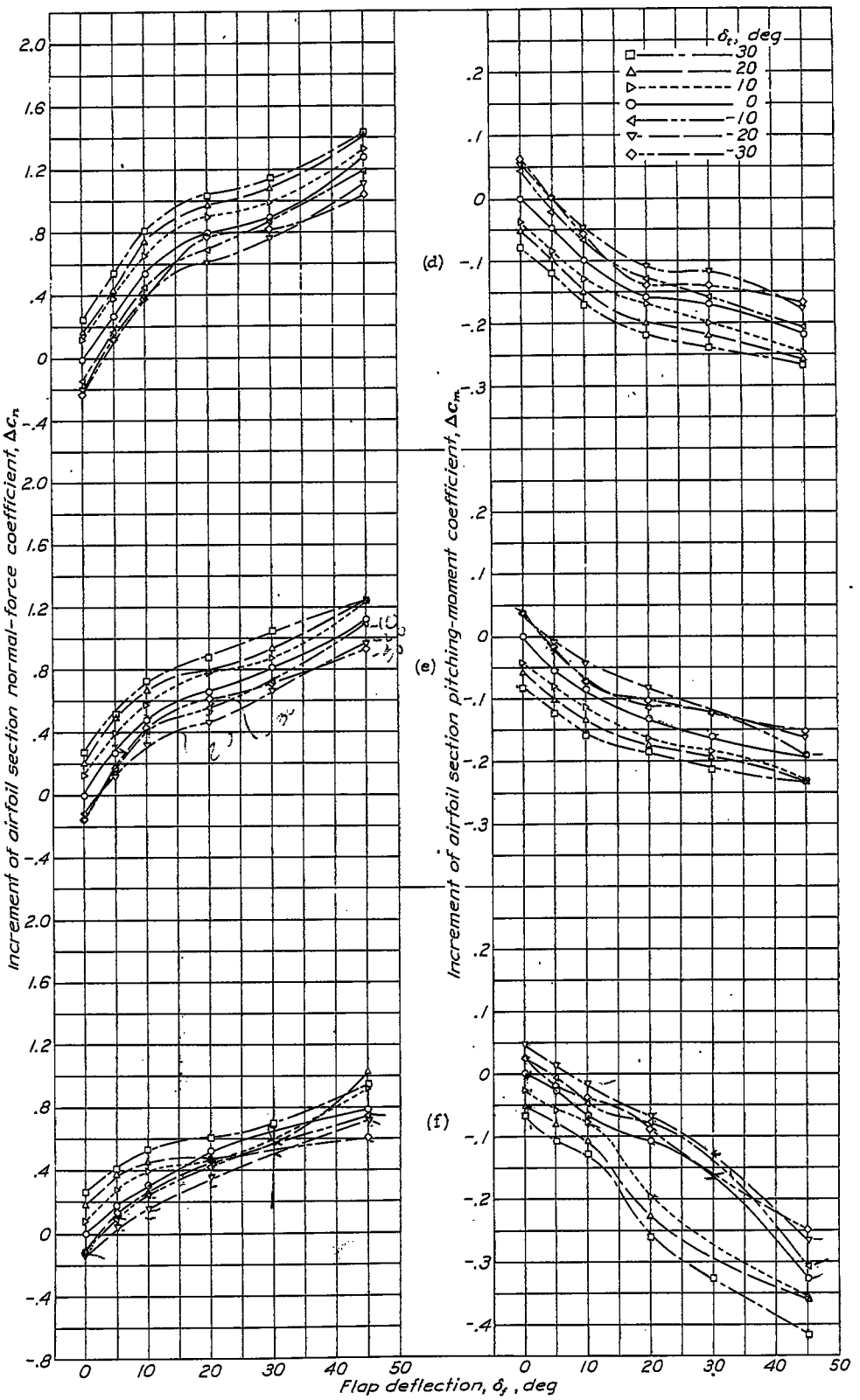

(d) α = 1/2° (e) α = 5 1/2° (f) α = 10 1/2°

Figure 12 concluded.

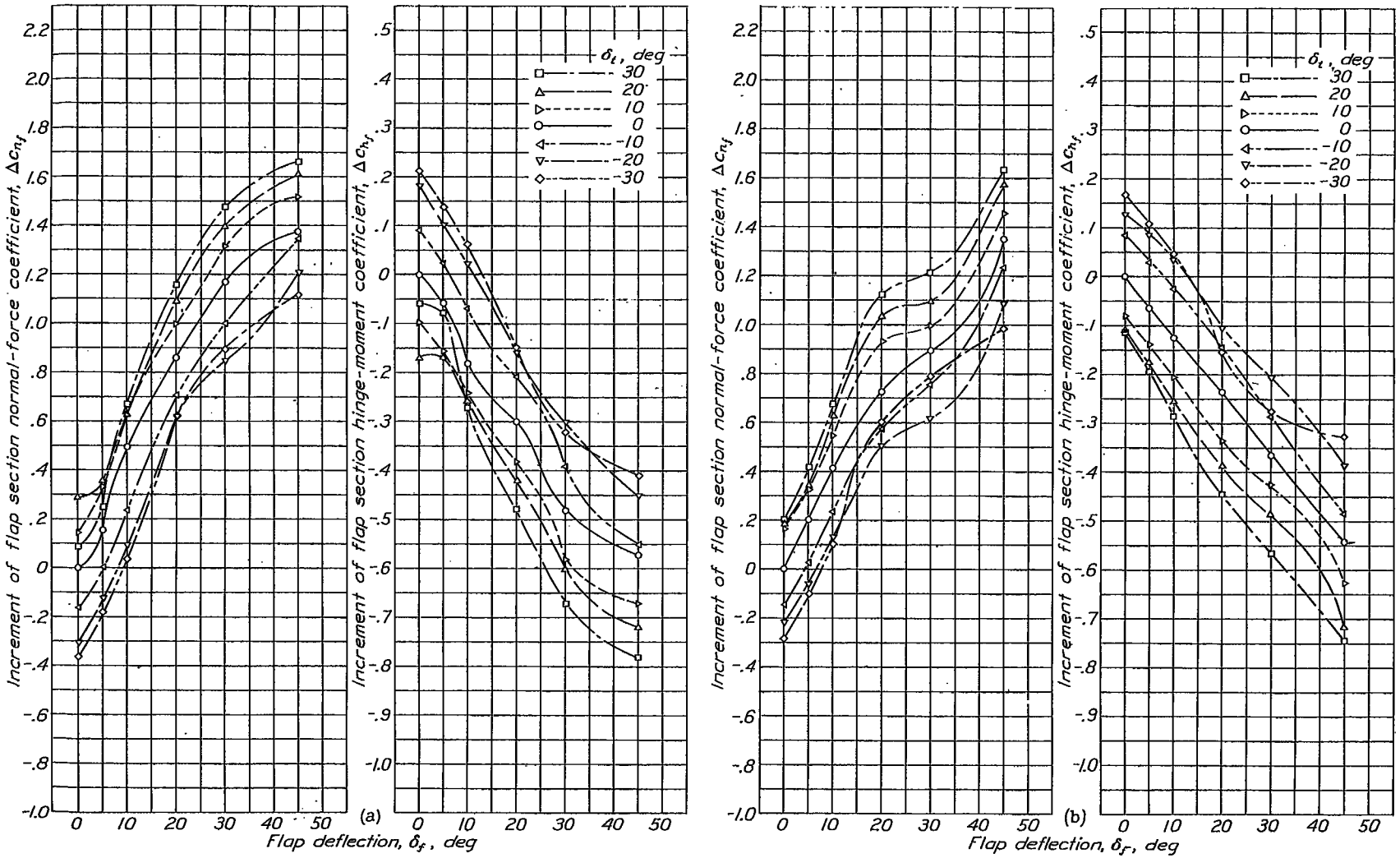

Figure 13, a to f.- Increments of flap section normal-force and hinge-moment coefficients for various deflections of a 0.30c plain flap and a $0.10c_f$ tab.

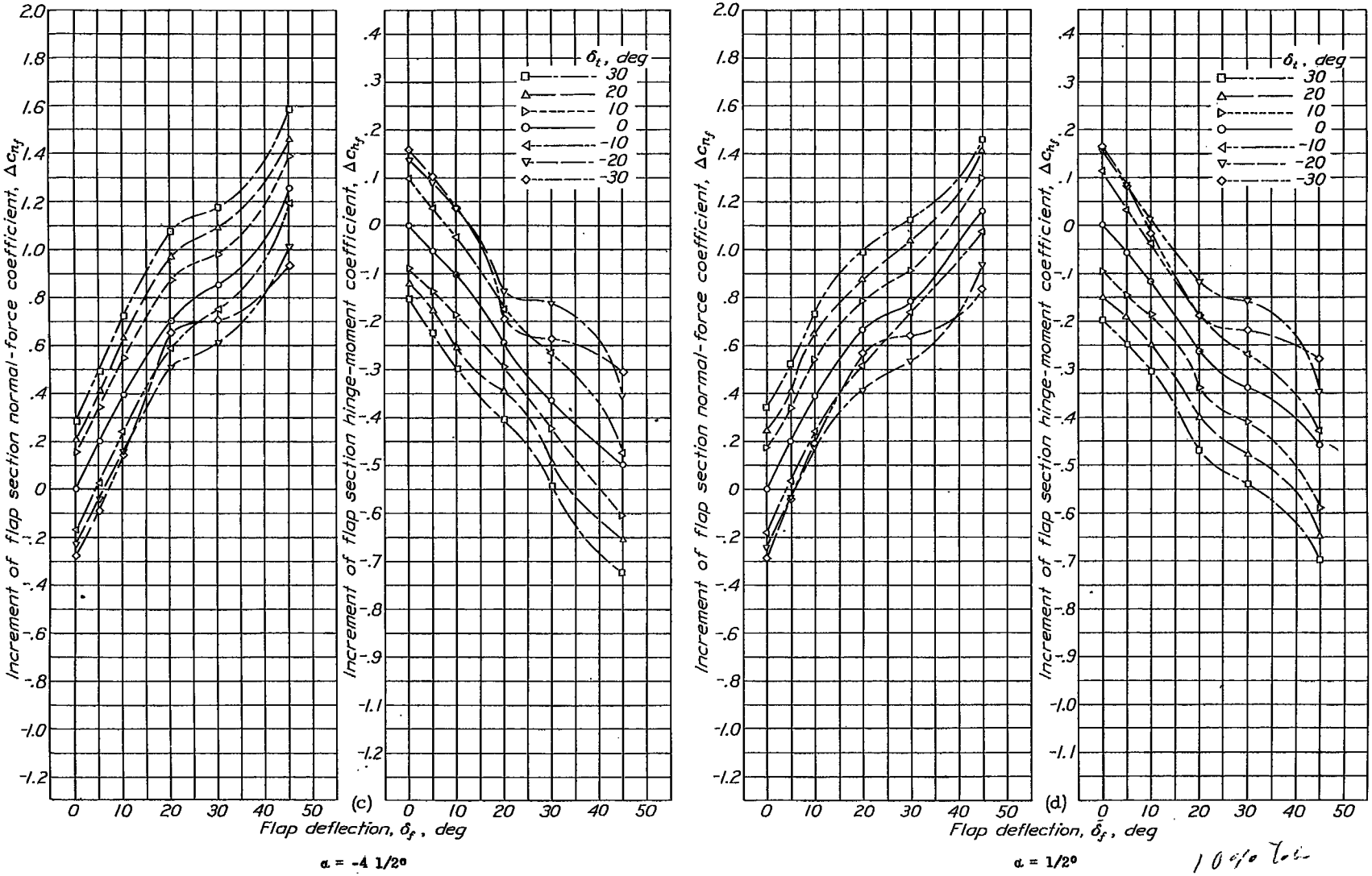

Figure 13 continued.

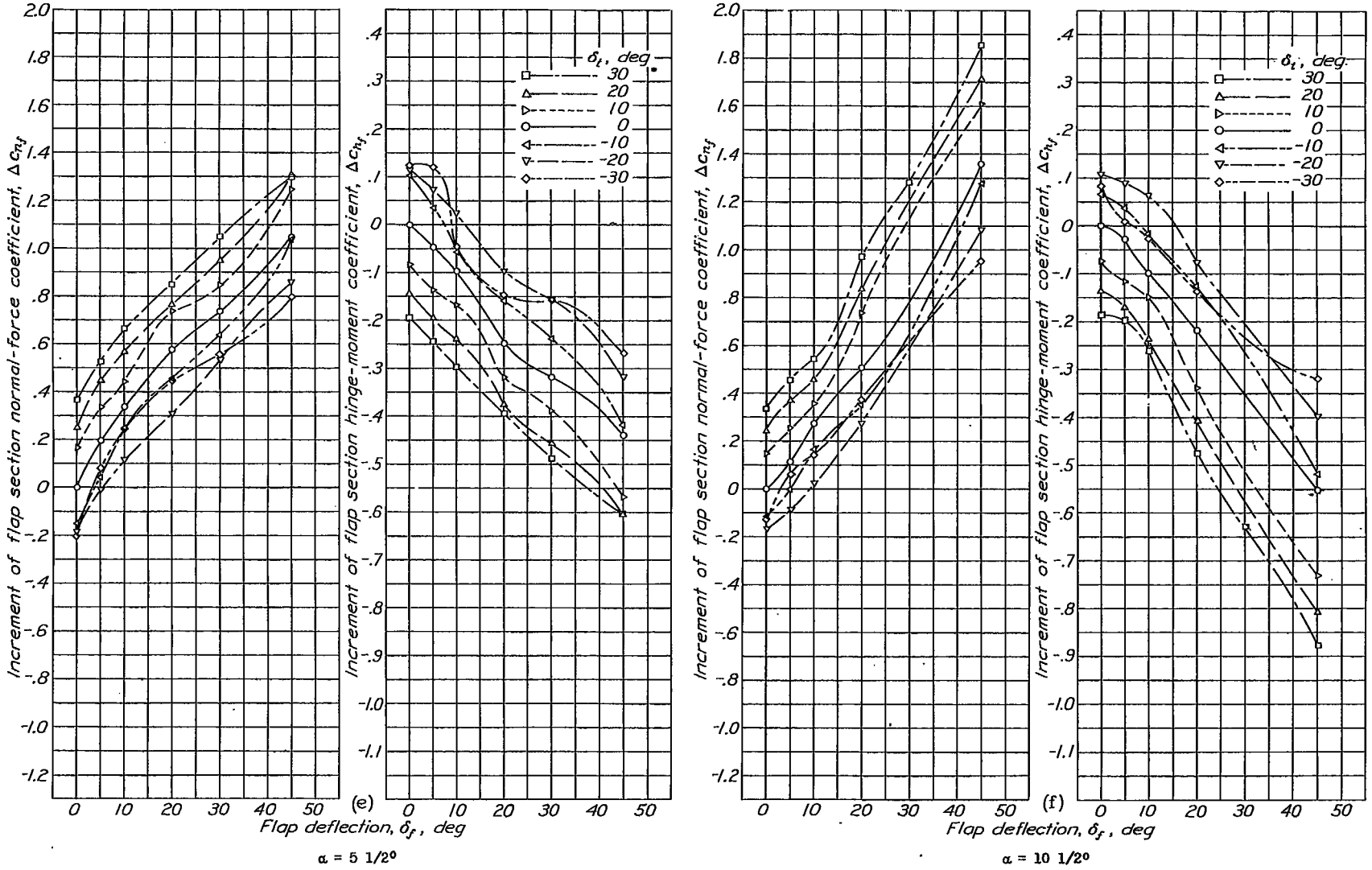

Figure 13 concluded.

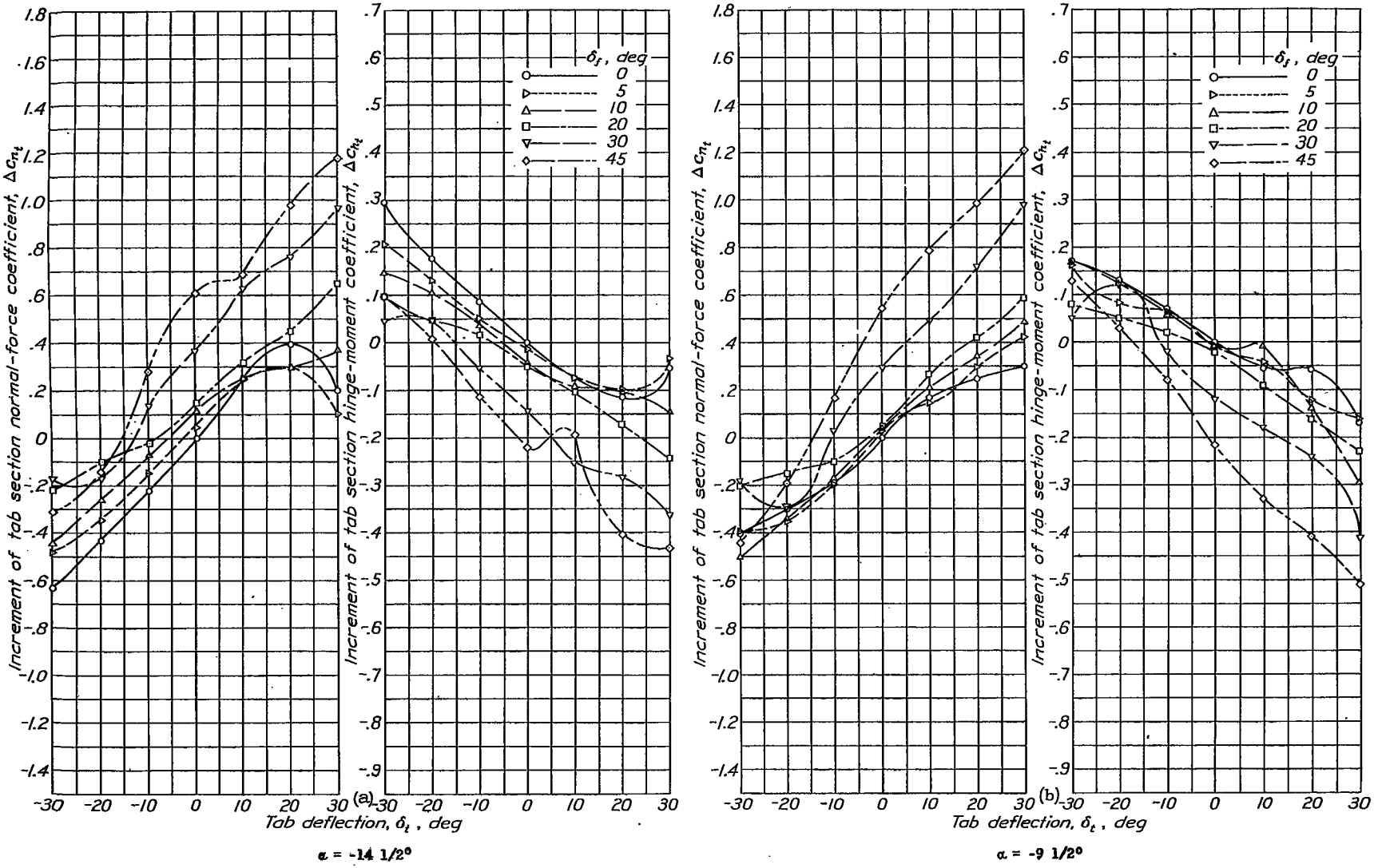

Figure 14, a to f.- Increments of tab section normal-force and hinge-moment coefficients for various deflections of a 0.30c plain flap and a 0.10c$_f$ tab.

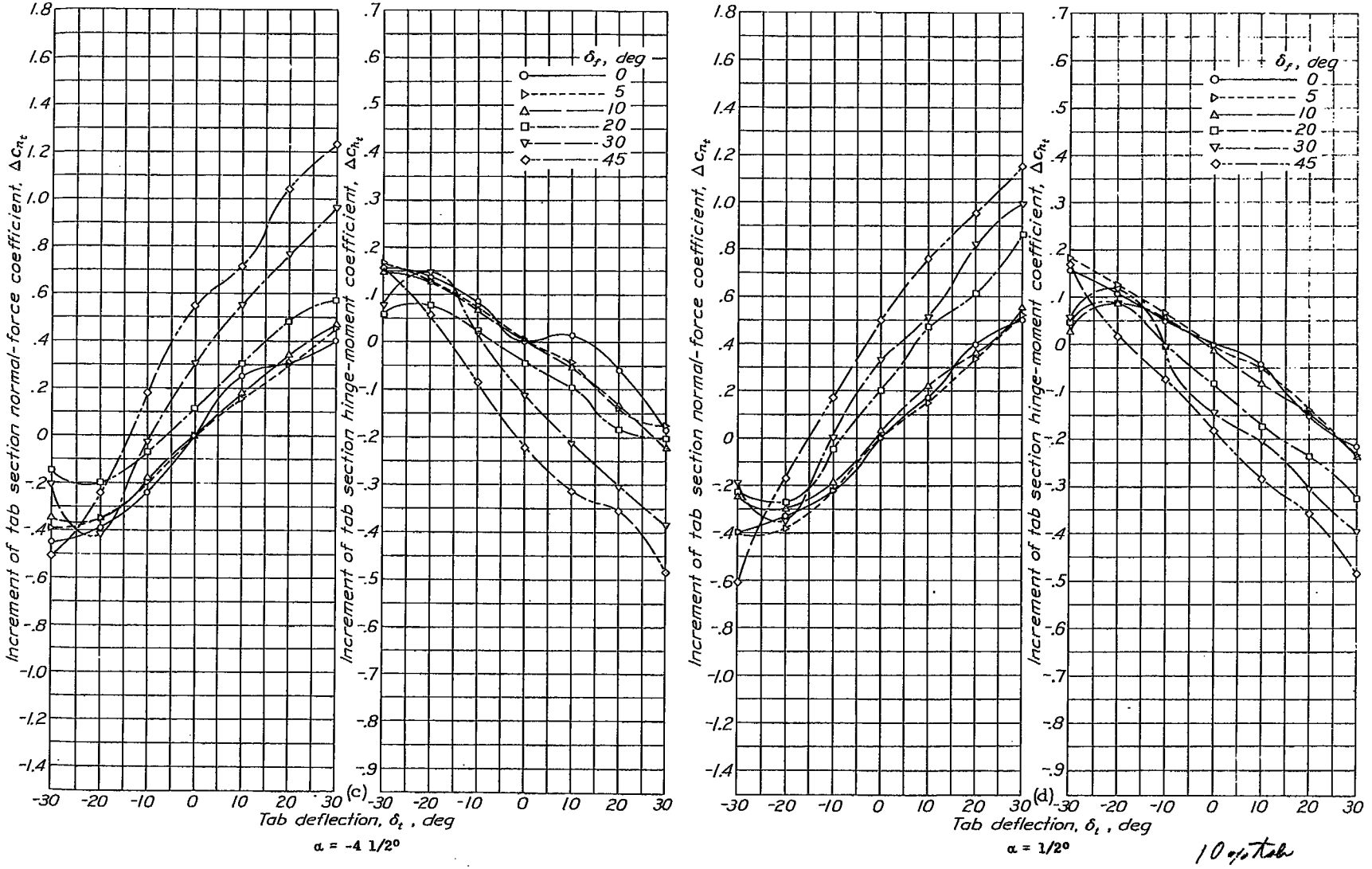

Figure 14 continued.

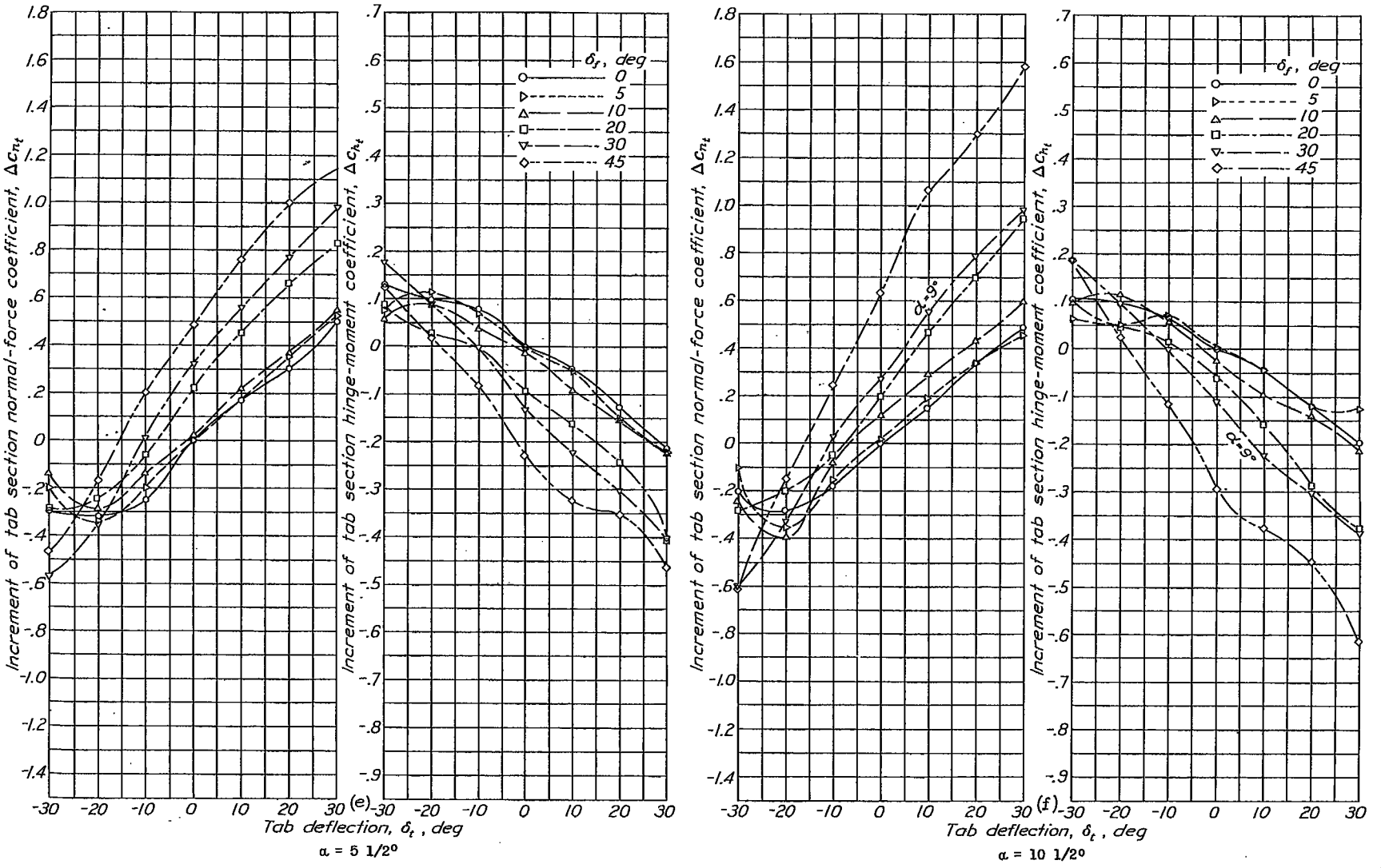

Figure 14 concluded.

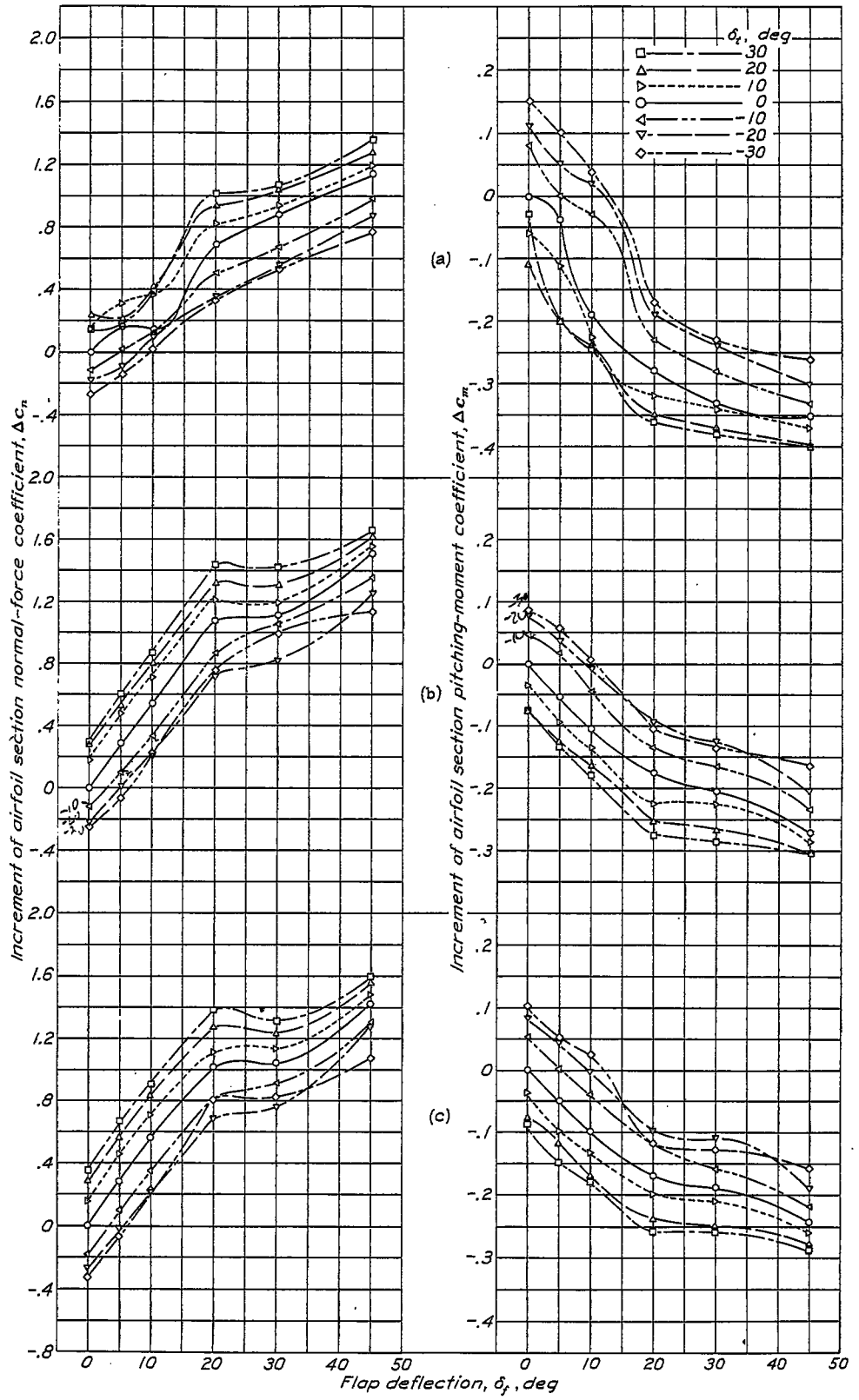

(a) α = -14 1/2° (b) α = -9 1/2° (c) α = -4 1/2°

Figure 15, a to f.- Increments of airfoil section normal-force and pitching-moment coefficients for various deflections of a 0.30c plain flap and a 0.20c_f tab.

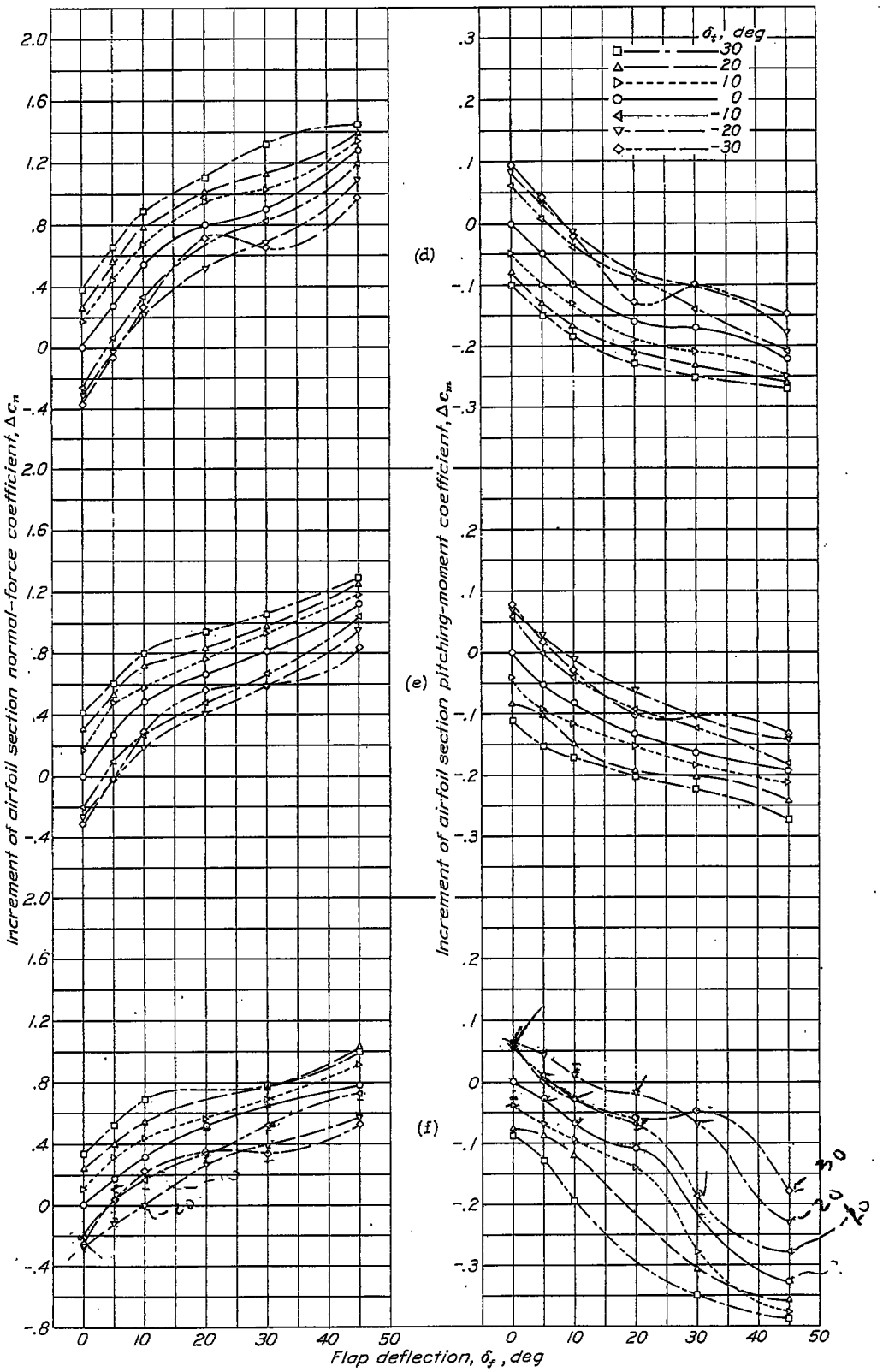

(d) α = 1/2° (e) α = 5 1/2° (f) α = 10 1/2°

Figure 15 concluded.

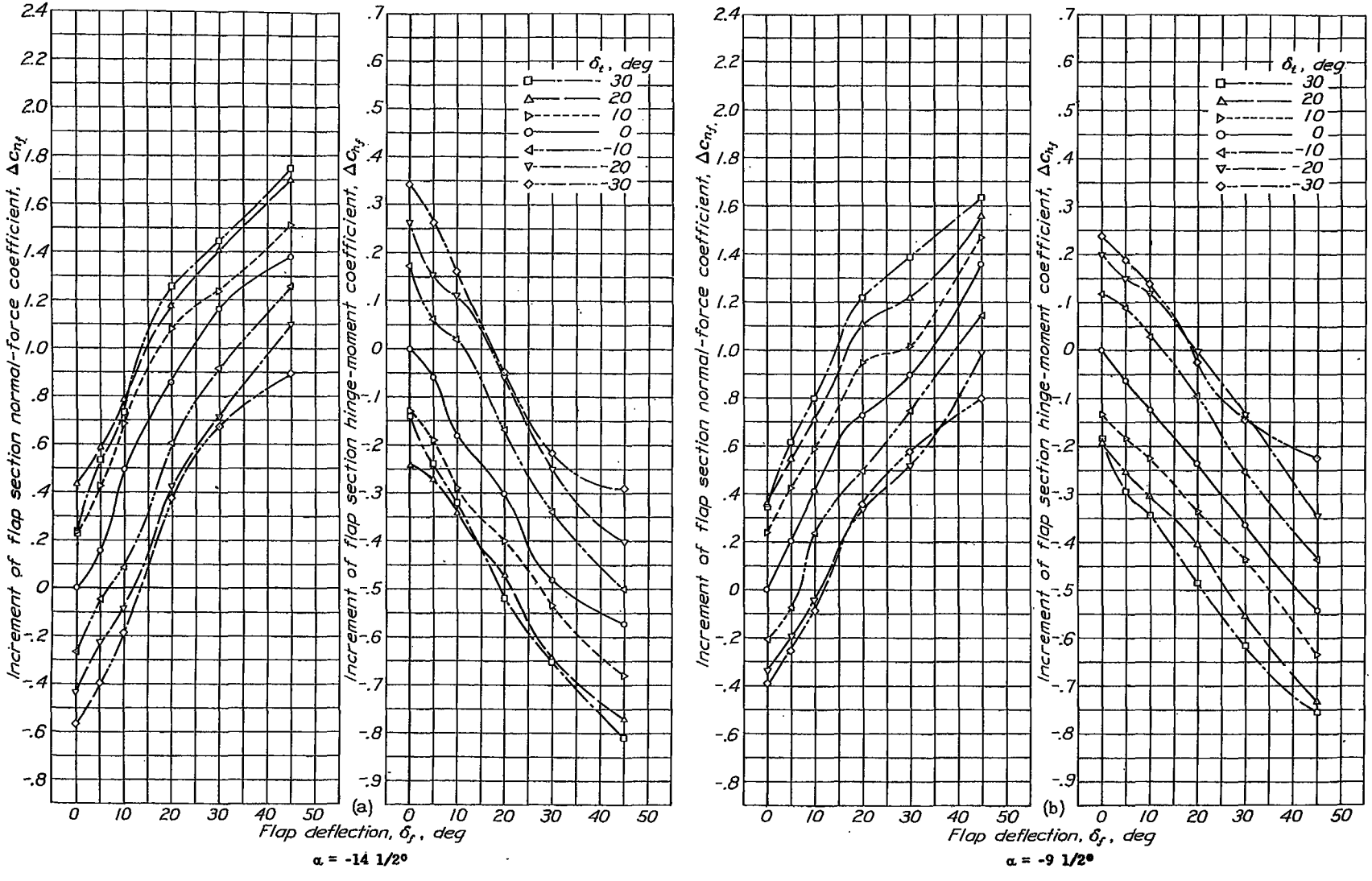

Figure 16, a to f.- Increments of flap section normal-force and hinge-moment coefficients for various deflections of a 0.30c plain flap and a 0.20c_f tab.

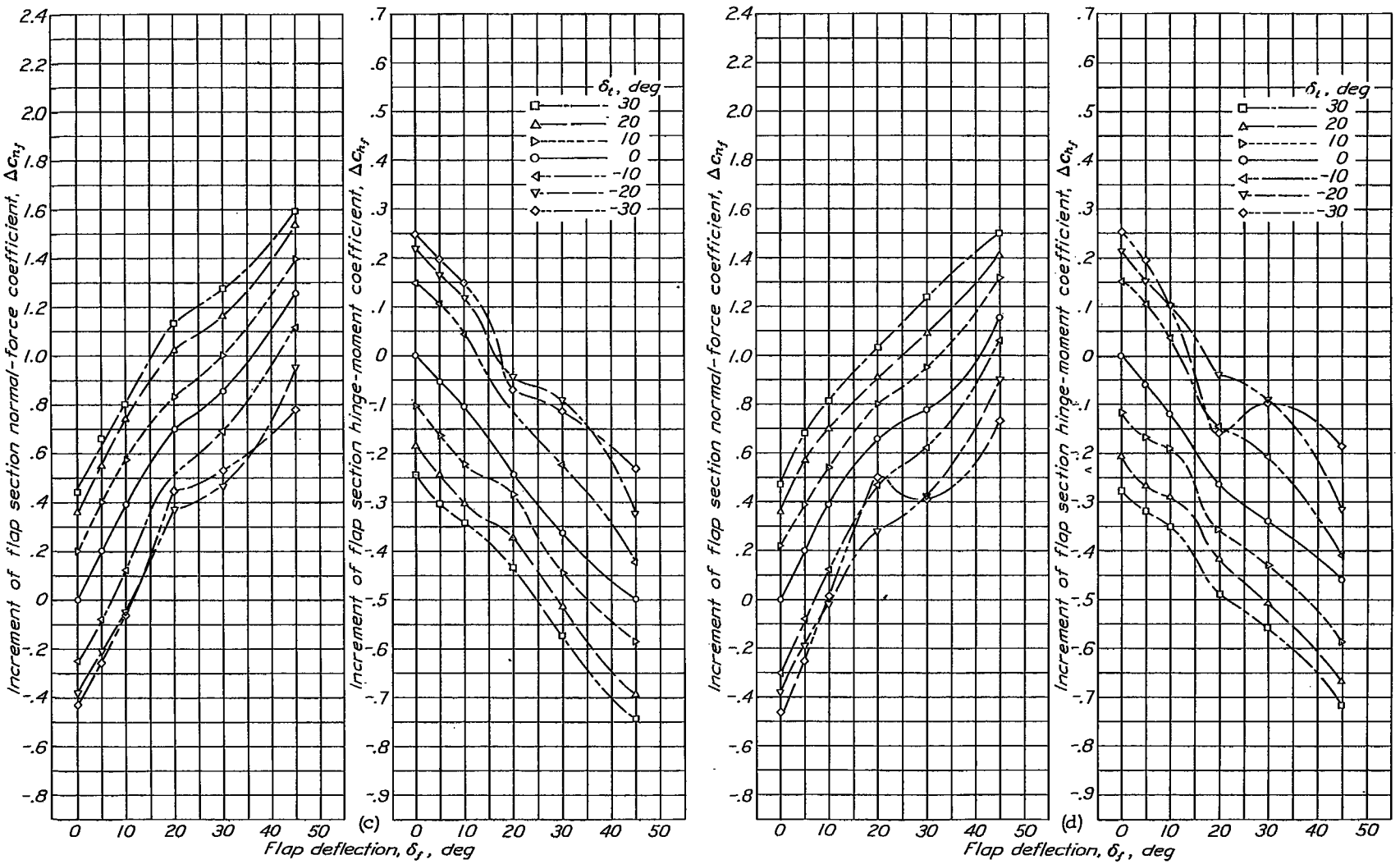

$\alpha = -4\ 1/2°$ $\alpha = 1/2°$

Figure 16 continued.

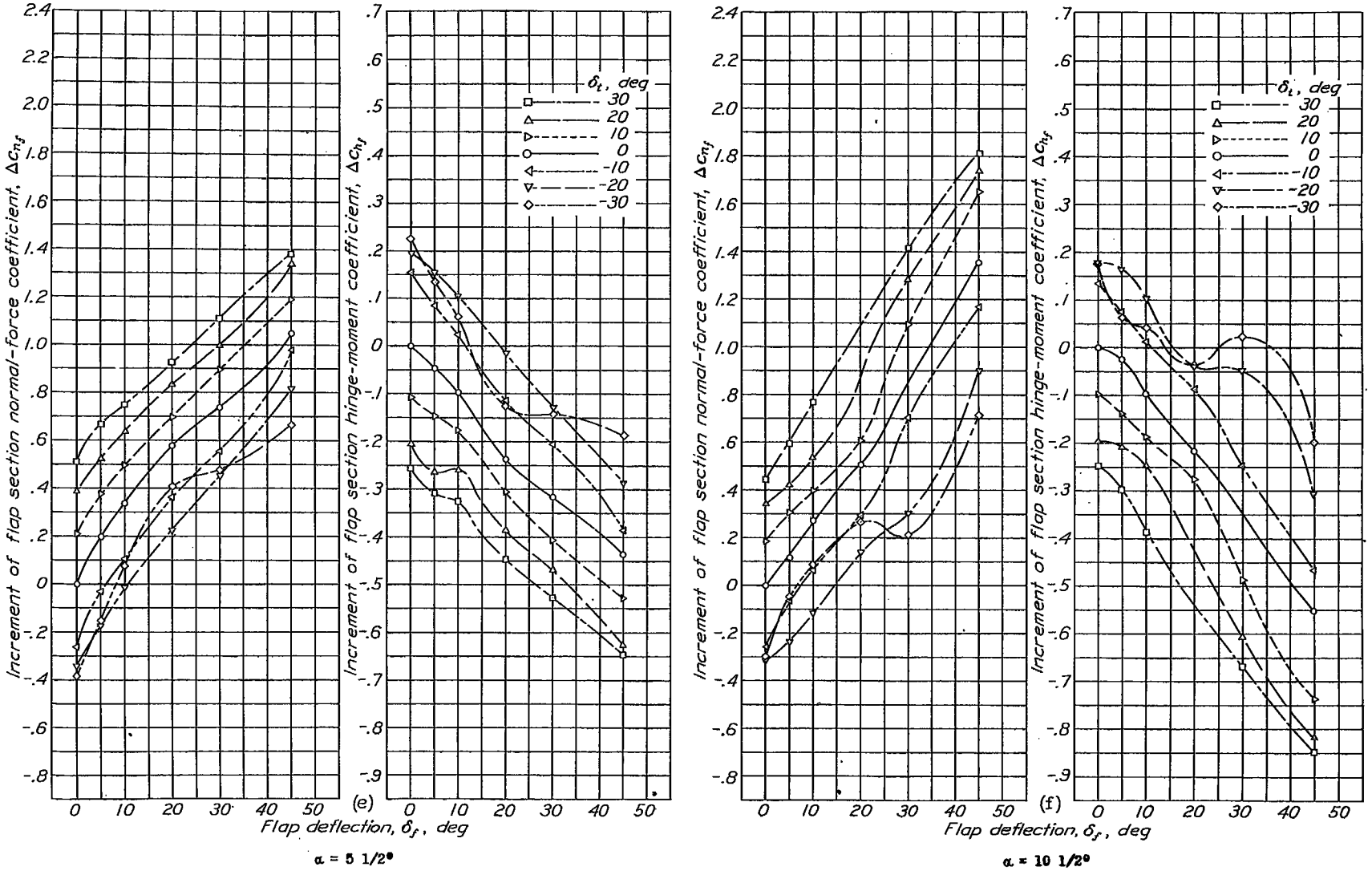

Figure 16 concluded.

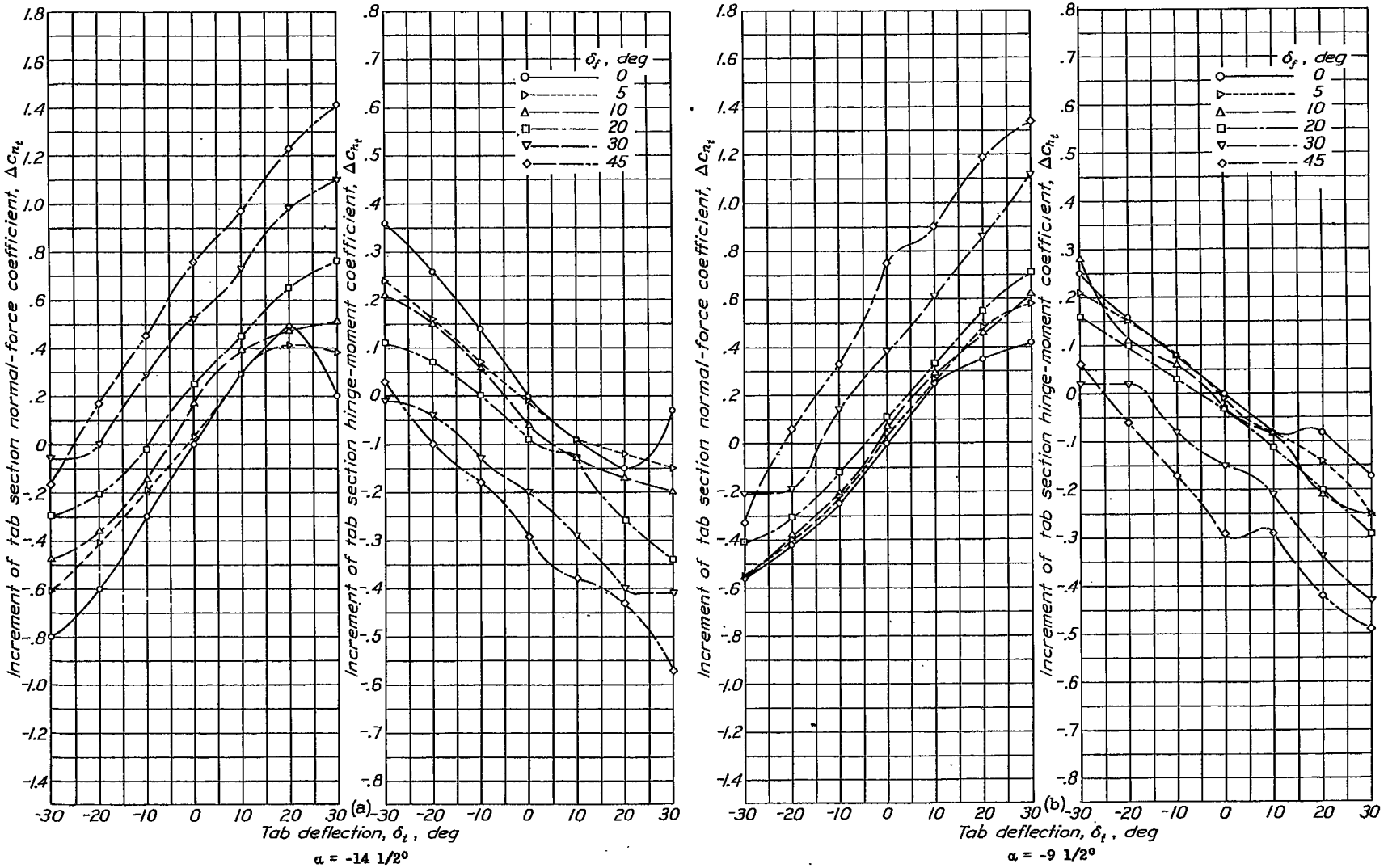

Figure 17, a to f.- Increments of tab section normal-force and hinge-moment coefficients for various deflections of a 0.30c plain flap and a 0.20c_f tab.

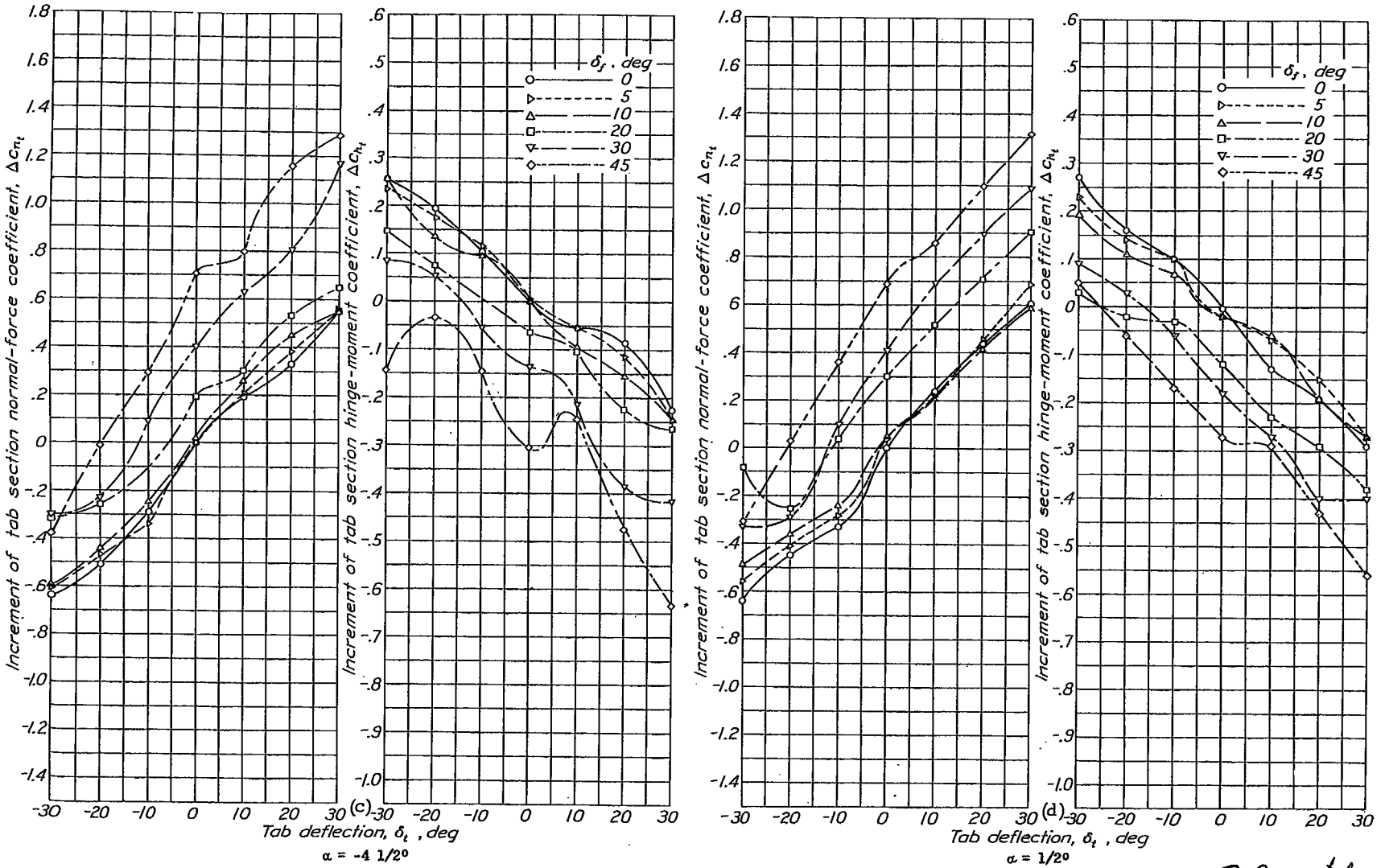

Figure 17 continued.

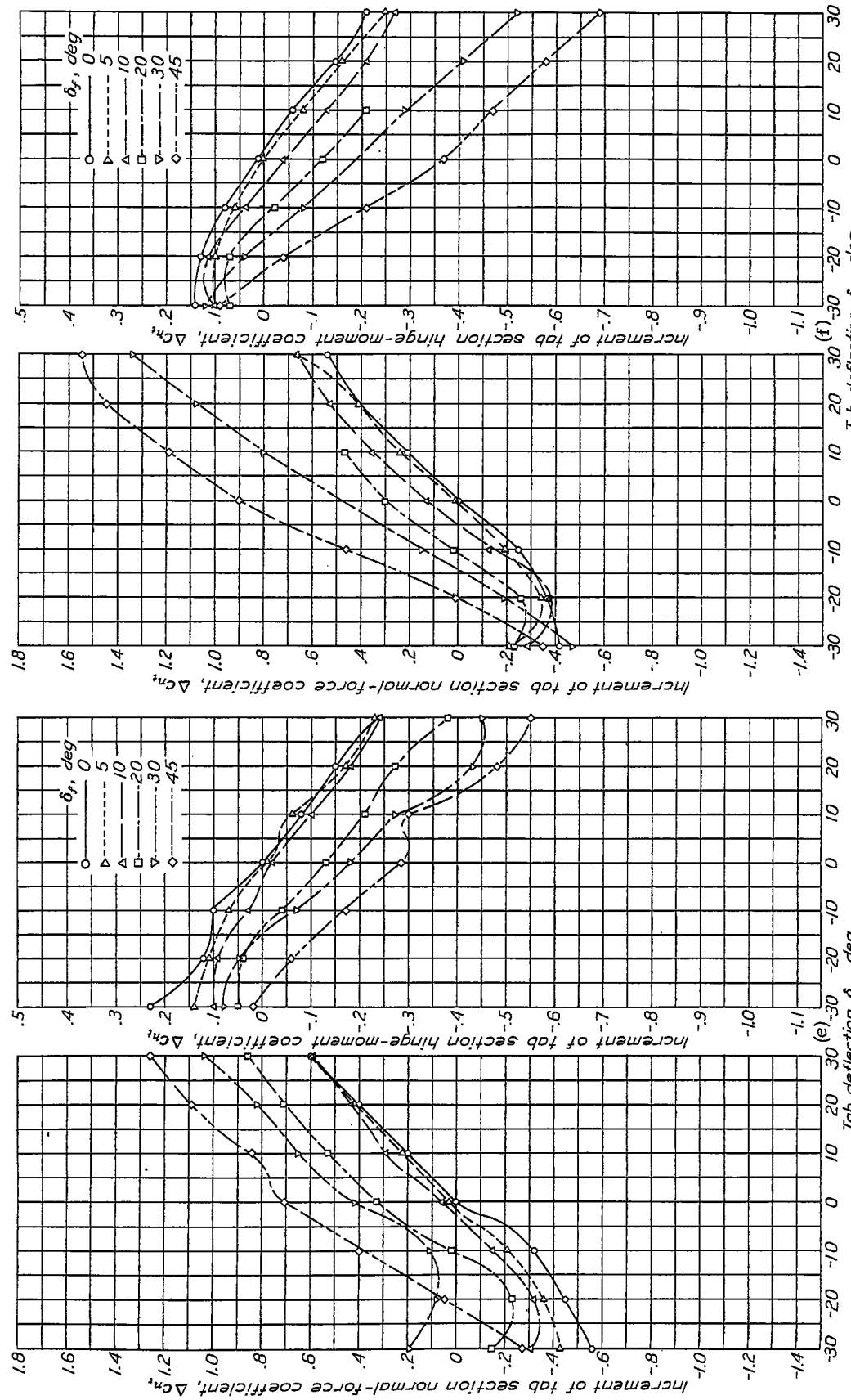

Figure 17 concluded.

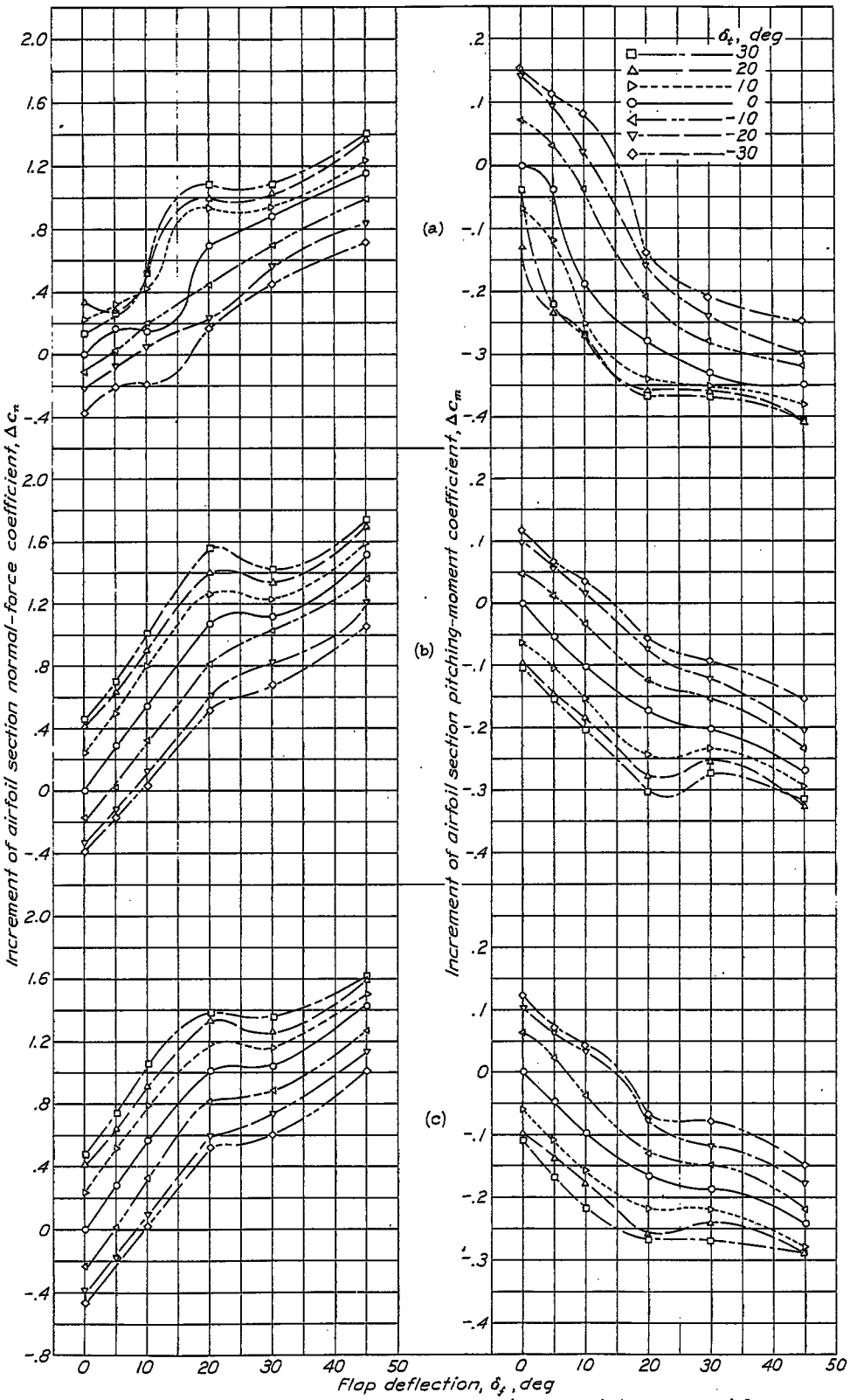

(a) α = -14 1/2° (b) α = -9 1/2° (c) α = -4 1/2°

Figure 18, a to f.- Increments of airfoil section normal-force and pitching-moment coefficients for various deflections of a 0.30c plain flap and a 0.30c_f tab.

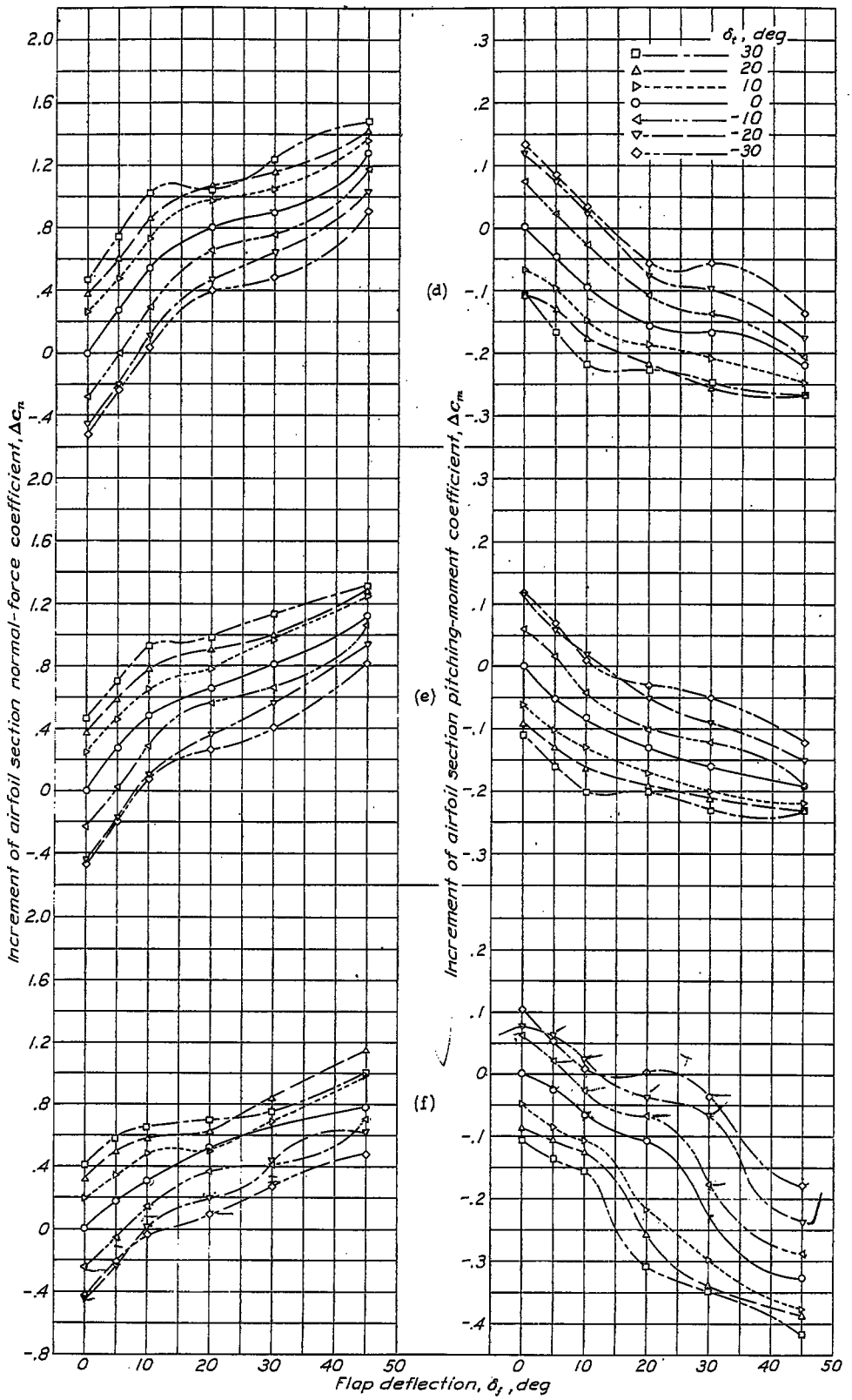

(d) α = 1/2° (e) α = 5 1/2° (f) α = 10 1/2°

Figure 18 concluded.

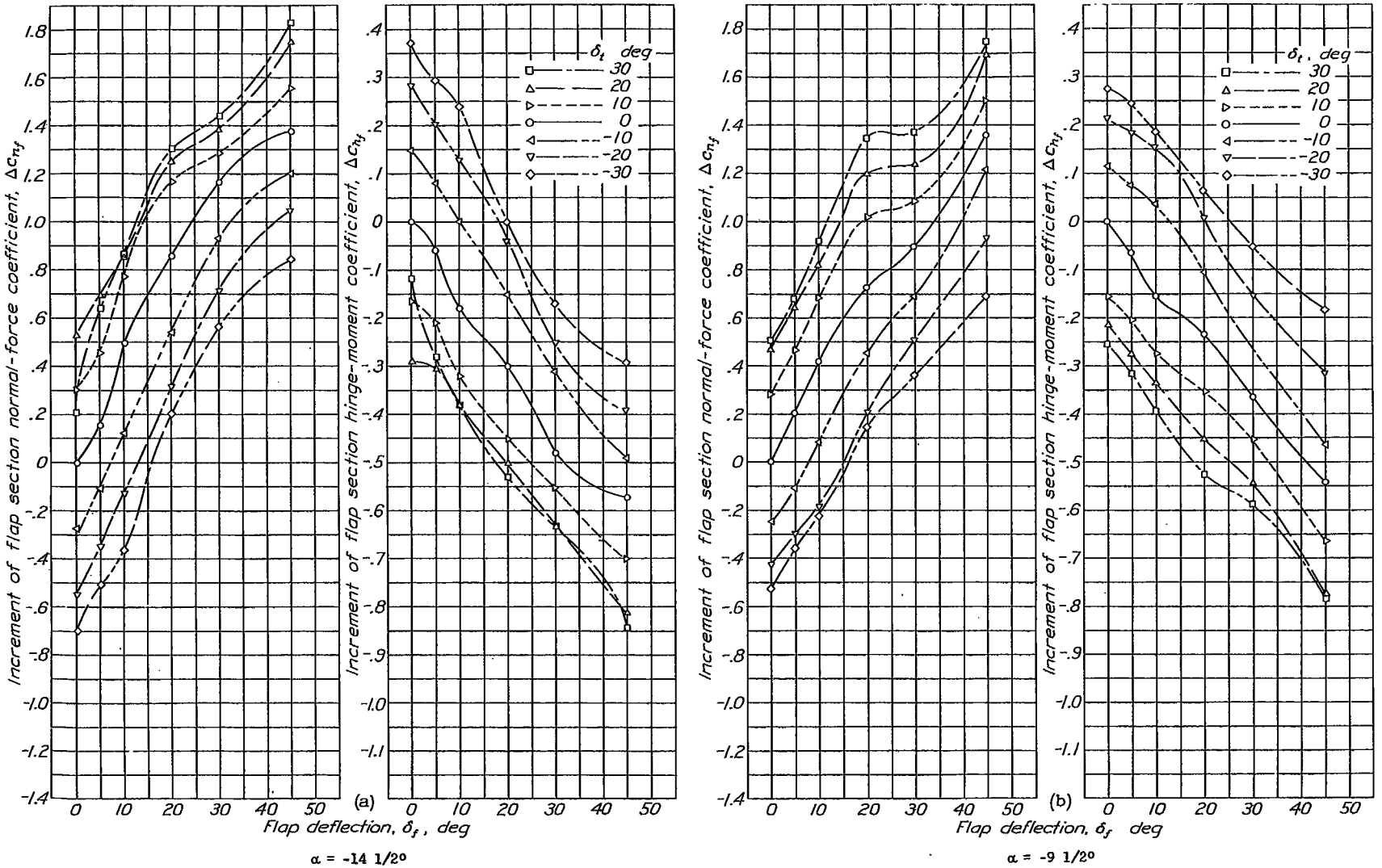

Figure 19, a to f.- Increments of flap section normal-force and hinge-moment coefficients for various deflections of a 0.30c plain flap and a 0.30c_f tab.

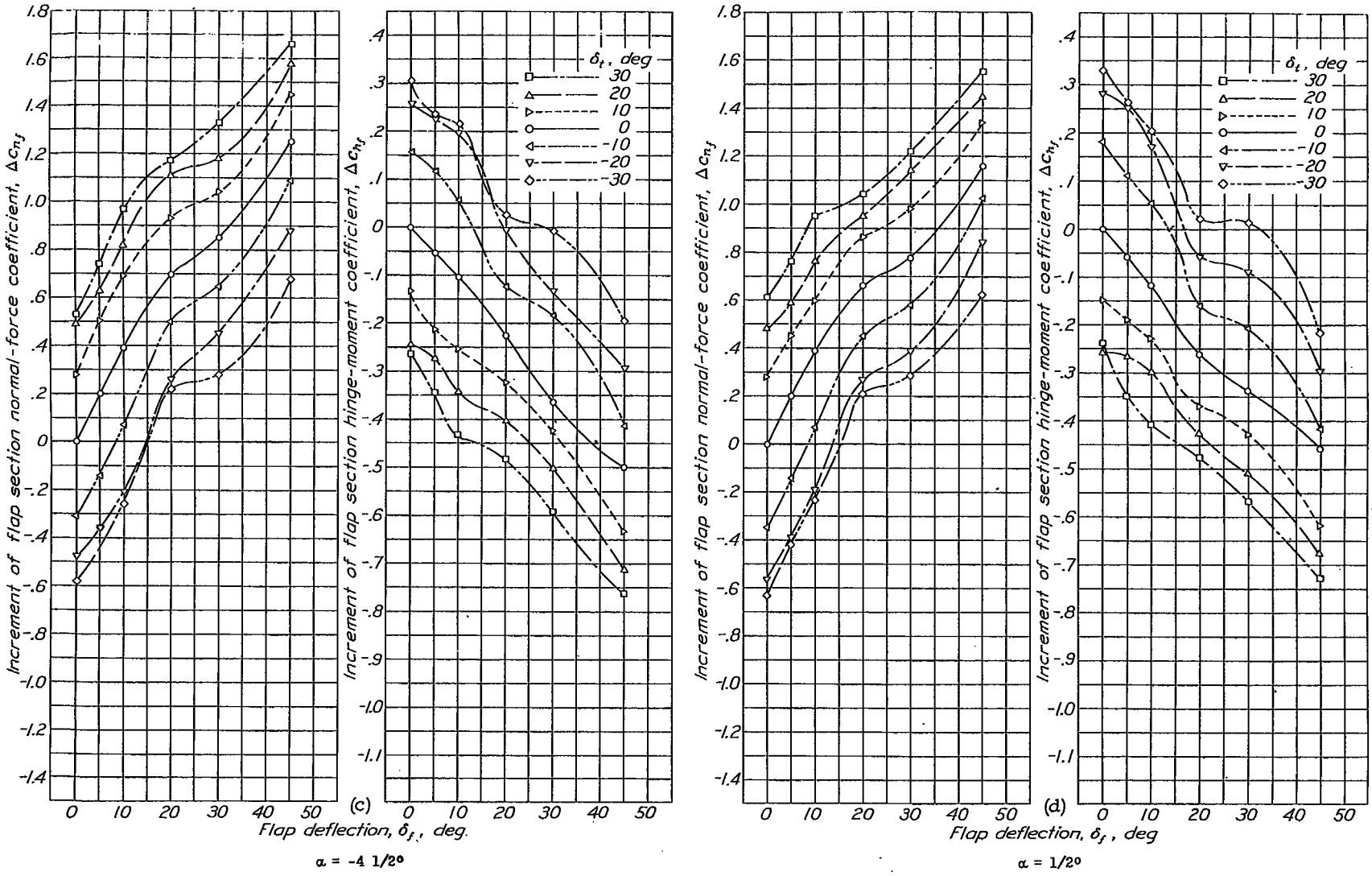

Figure 19 continued.

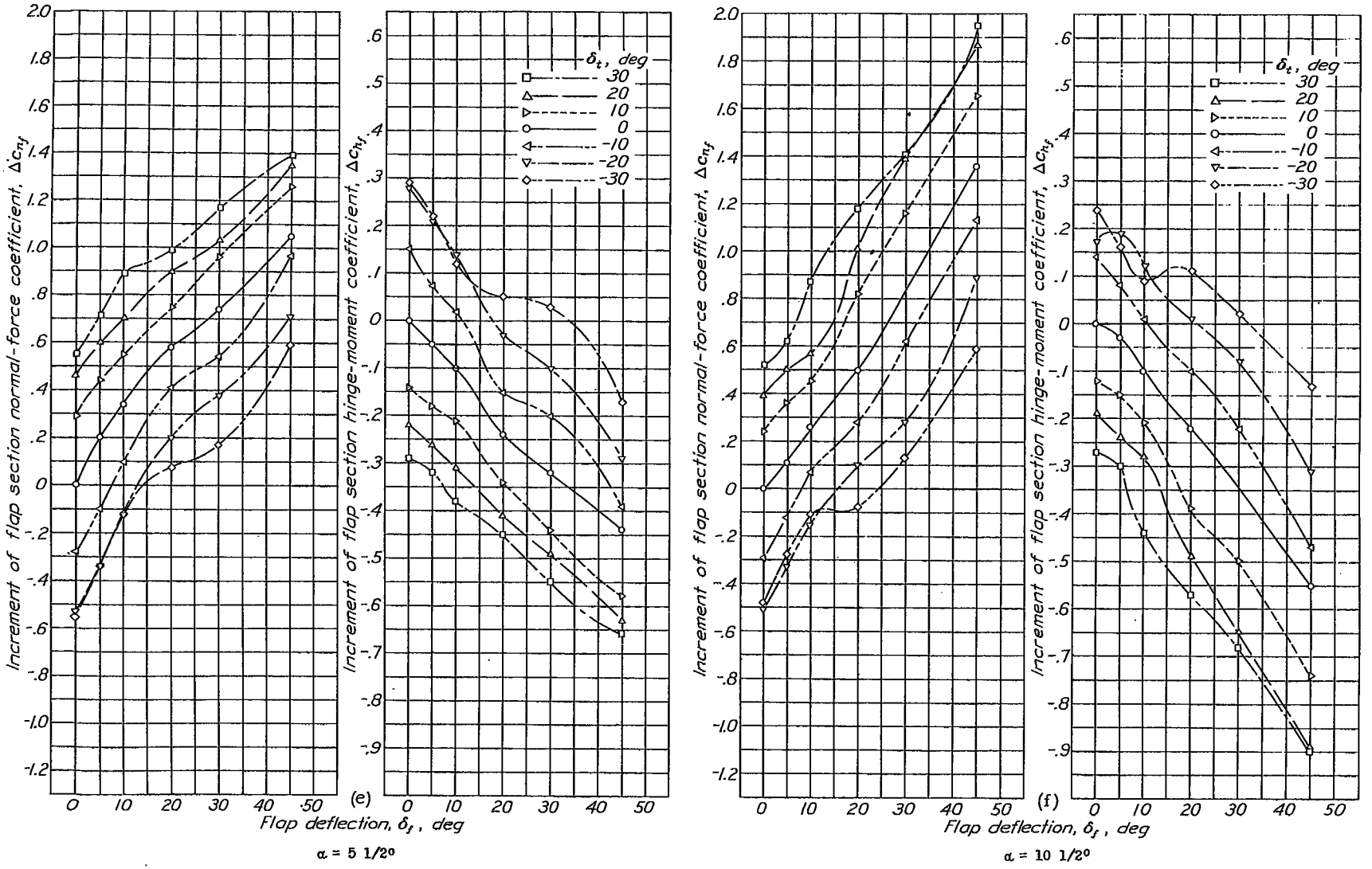

Figure 19 concluded.

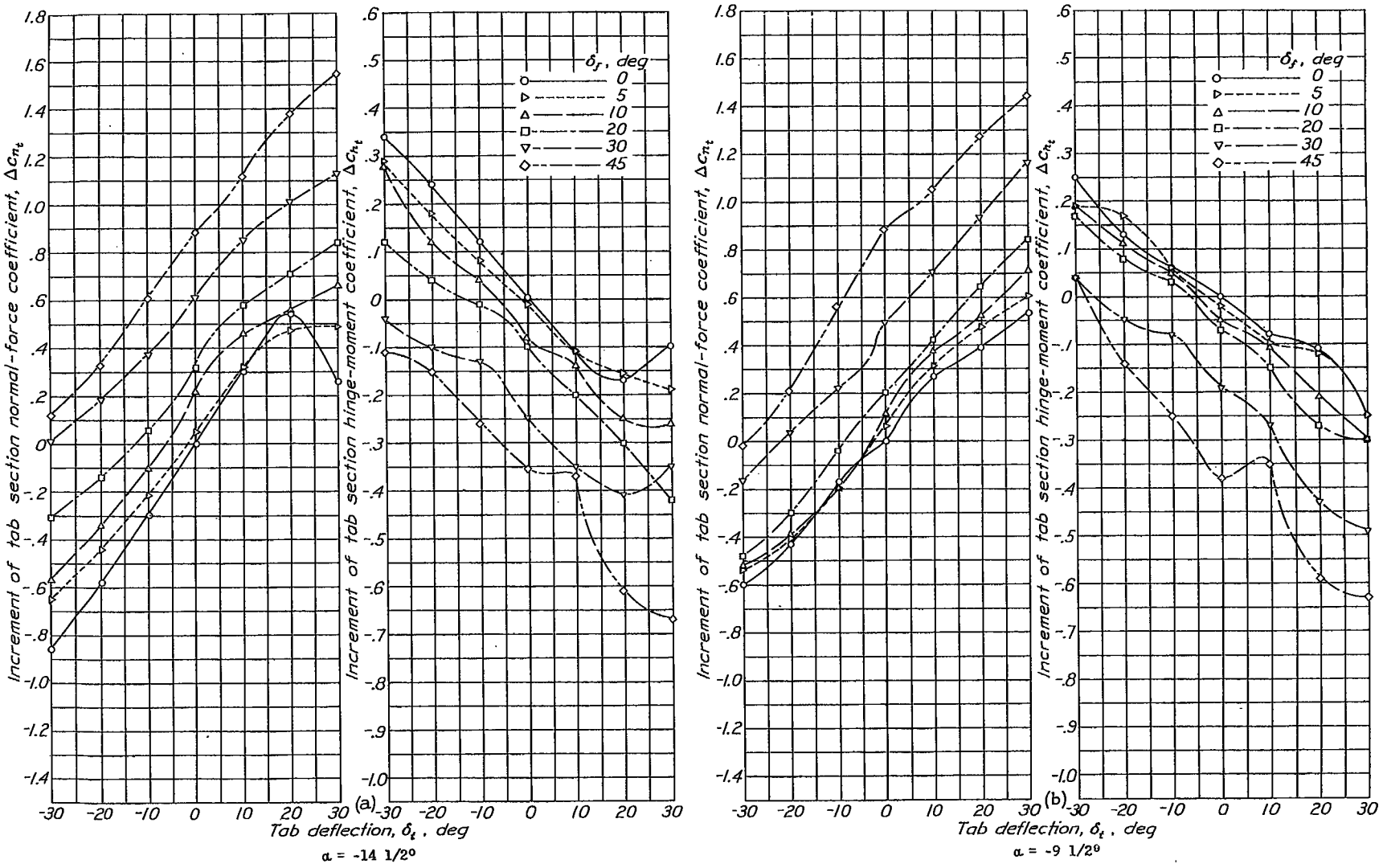

Figure 20, a to f.- Increments of tab section normal-force and hinge-moment coefficients for various deflections of a 0.30c plain flap and a 0.30c_f tab.

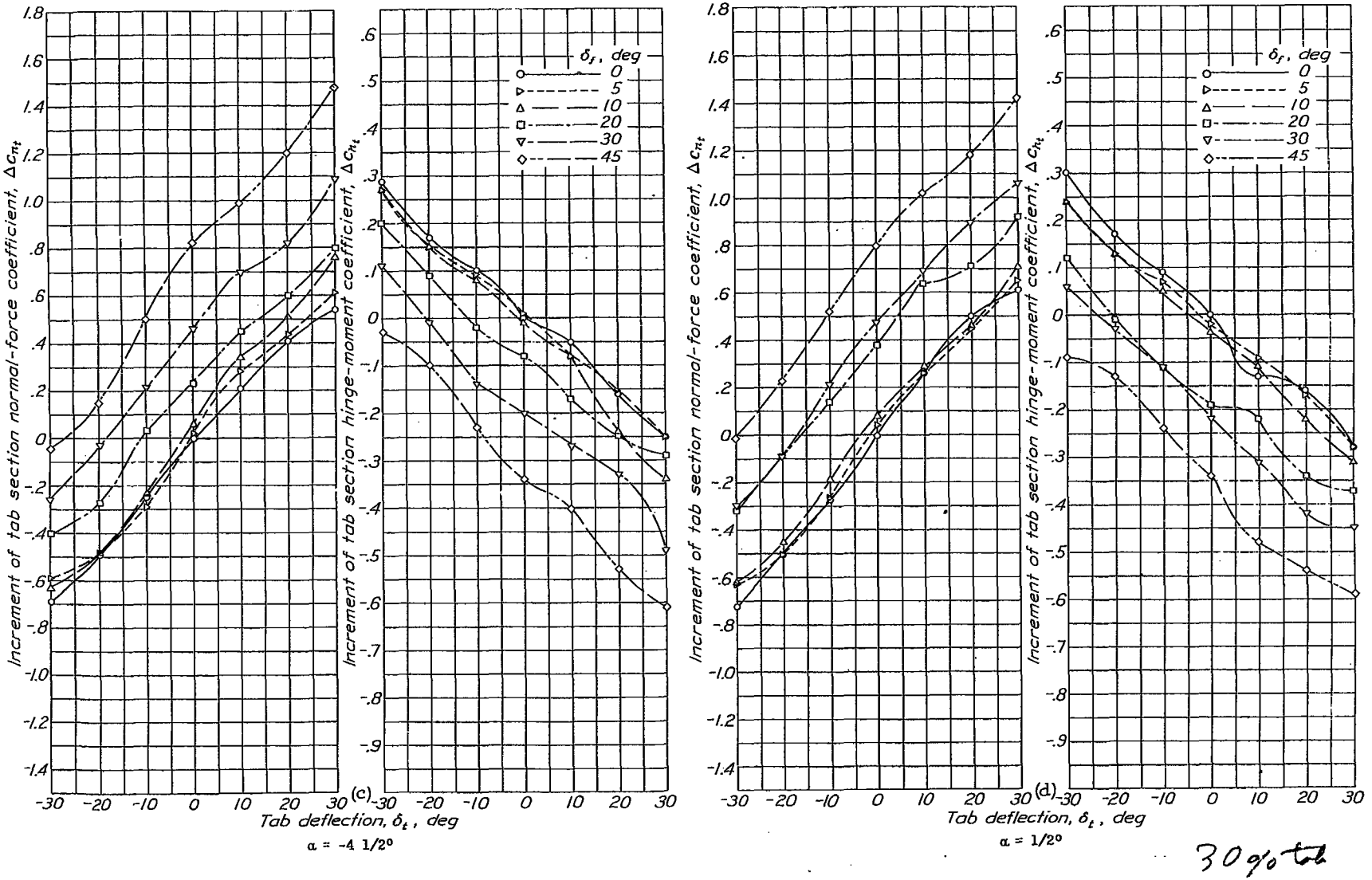

Figure 20 continued.

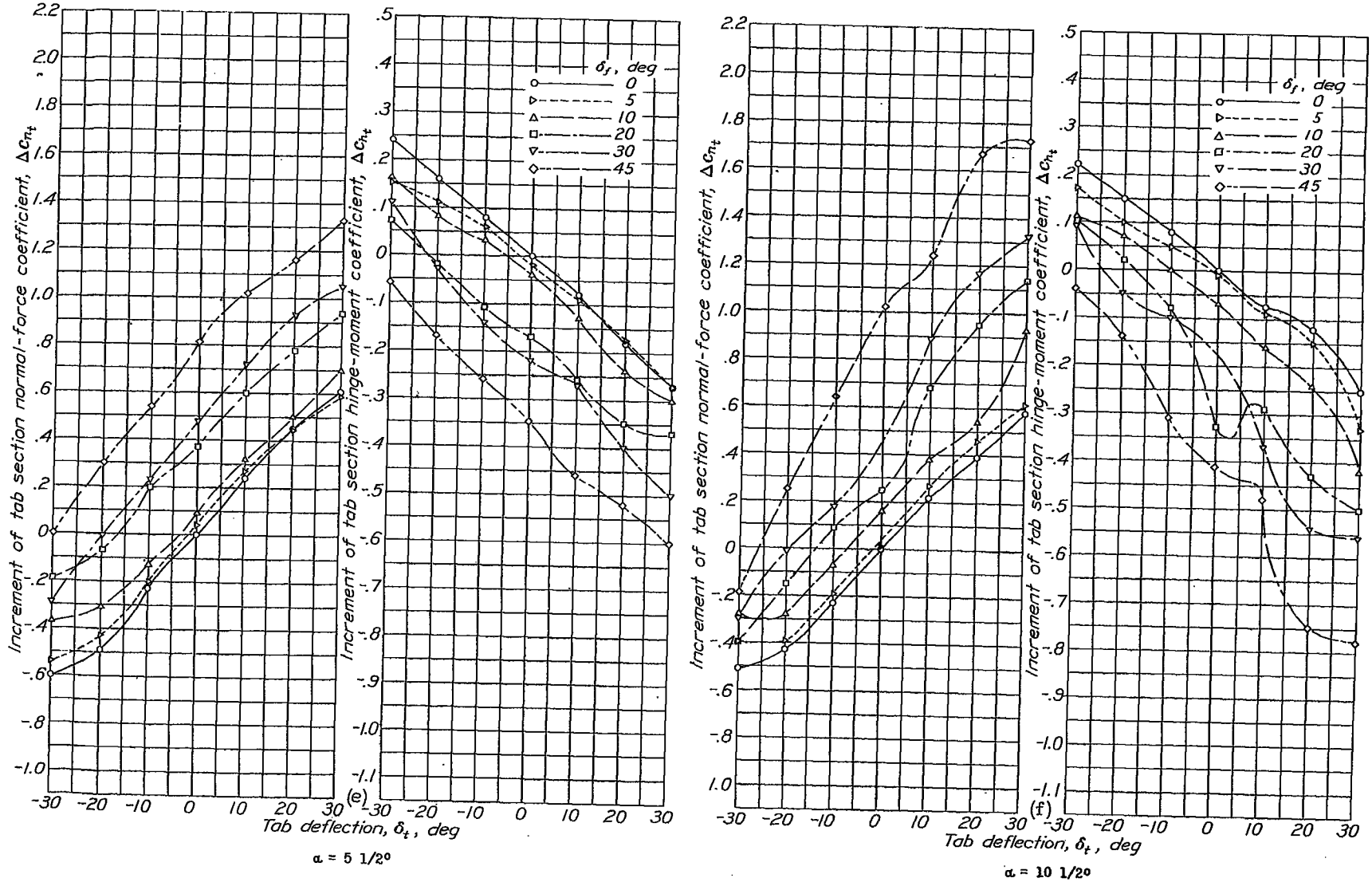

Figure 20 concluded.